Hindawi Publishing Corporation
Shock and Vibration
Volume 2015, Article ID 148681, 22 pages
http://dx.doi.org/10.1155/2015/148681

Research Article

On the Design of High-Rise Buildings for Multihazard: Fundamental Differences between Wind and Earthquake Demand

Aly Mousaad Aly and Srinivasa Abburu

Department of Civil and Environmental Engineering, Louisiana State University, Baton Rouge, LA 70803, USA

Correspondence should be addressed to Aly Mousaad Aly; aly@LSU.edu

Received 10 December 2014; Revised 13 May 2015; Accepted 18 June 2015

Academic Editor: Alicia Gonzalez-Buelga

In the past few decades, high-rise buildings have received a renewed interest in many city business locations, where land is scarce, as per their economics, sustainability, and other benefits. Taller and taller towers are being built everywhere in the world. However, the increased frequency of multihazard disasters makes it challenging to balance between a resilient and sustainable construction. Accordingly, it is essential to understand the behavior of such structures under multihazard loadings, in order to apply such knowledge to design. The results obtained from the dynamic analysis of two different high-rise buildings (54-story and 76-story buildings) investigated in the current study indicate that earthquake loads excite higher modes that produce lower interstory drift, compared to wind loads, but higher accelerations that occur for a shorter time. Wind-induced accelerations may have comfort and serviceability concerns, while excessive interstory drifts can cause security issues. The results also show that high-rise and slender buildings designed for wind may be safe under moderate earthquake loads, regarding the main force resisting system. Nevertheless, nonstructural components may present a significant percentage of loss exposure of buildings to earthquakes due to higher floor acceleration. Consequently, appropriate damping/control techniques for tall buildings are recommended for mitigation under multihazard.

1. Introduction

(1) Background. Wind and seismic hazards, coupled with aging and vulnerable buildings, pose the potential for damage and loss of life and property. Both hazards can wreak catastrophic damage to buildings and the infrastructure in general. Hurricane winds and earthquakes cause the majority of insured property loss in the world from all natural disasters. Although an individual hazard may be more significant than the other, the rapid population growth and economic development have greatly increased the potential of exposure to multiple hazards [1]. Current design codes and hazard mitigation strategies treat hurricanes and earthquakes as completely independent, which does not account for the increased risk to structures in regions where both hazards are present [2].

Buildings are usually subjected to static loads, such as occupants' weight, equipment, furniture, and the weight of the structure. However, two important environmental loads that are different in nature may attack our buildings once or twice during their lifetime. The nature of the two loads is totally different from the static load, and even if they could be expressed as equivalent static loads, tall buildings and flexible structures may amplify the internal loads resulting in additional inertia loads which can alarm the serviceability and the comfort concern of people in a building or even lead to a complete collapse. When it comes to dynamics and load-structure interaction, the inherently low damping in buildings is a key parameter that can be used to control the behavior of a structure under such dynamic loads. In addition, building's orientation change can result in wind response/load reduction. High-rise buildings are an increasingly common sight because they provide a high ratio of rentable floor space per unit area of land, in addition to other factors, such as architectural and energy perspectives. Tall buildings or "skyscrapers" can be artificially lighted and

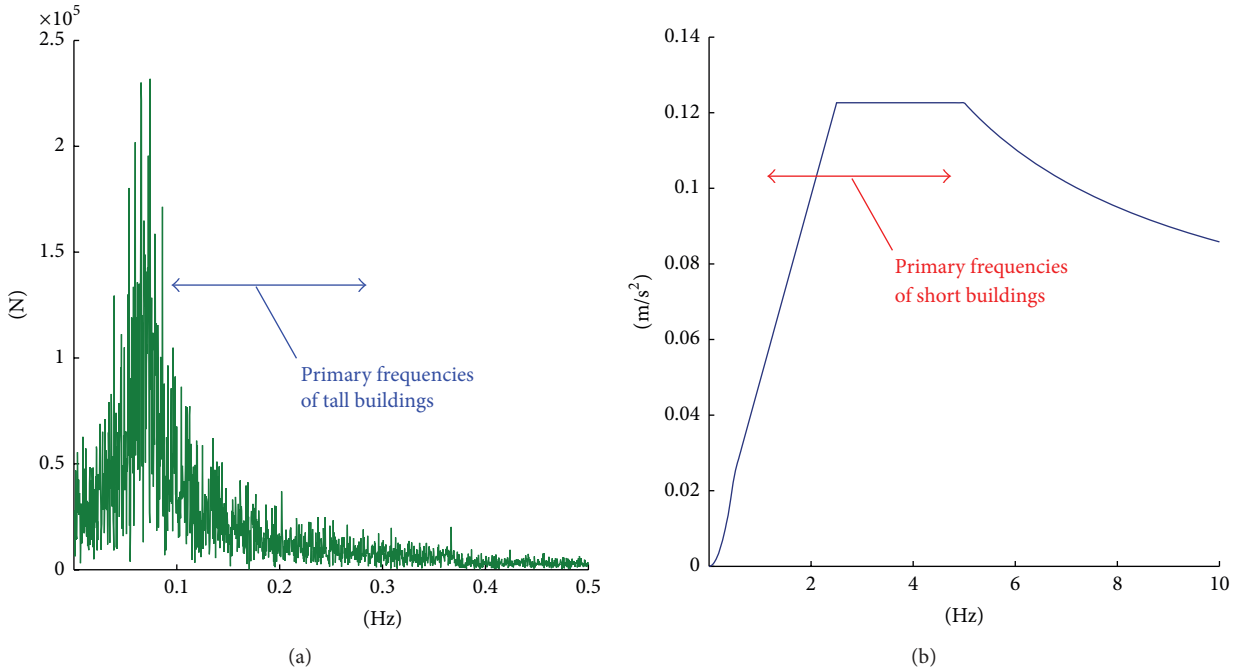

Figure 1: Spectra of wind and earthquake loads: (a) crosswind loads and (b) ground acceleration.

the energy requirements can be covered by renewable energy or another electricity generation of lower greenhouse gas emissions. Heating and cooling of skyscrapers can be efficient, because of centralized HVAC systems, heat radiation blocking windows, and small surface area of the building. There is a Leadership in Energy and Environmental Design (LEED) certification for skyscrapers. For instance, the Empire State Building received a gold rating in September 2011 as the tallest LEED certified building in the United States [3]. Also, the 30 St Mary Axe (the Gherkin) in London, the United Kingdom, is an environmentally friendly skyscraper [4].

On the other hand, developments in structural materials and design technology in civil engineering have led to designs that satisfy strength requirements but are often flexible. This flexibility can cause unfavorable vibrations when the structure is subjected to wind or earthquake loads. These vibrations may lead to serious structural damage and affect the comfort of the occupants. Dynamics of buildings greatly depends on the characteristics of the external excitation as well as the physical properties of the building in terms of generalized masses, frequencies, and damping. Wind loads are characterized by low frequencies while earthquakes usually contain higher frequency load components.

Figure 1 shows general spectra of wind and earthquake loads. Most of the dynamics-associated damage and discomfort in buildings are referred to excitations close to first few modes. In super tall buildings, however, first modes are likely to have low frequencies which make them mostly affected by wind loads rather than earthquakes. On the opposite side, short buildings suffered much from dynamics-associated damage under earthquake loads which likely occurs at the dominant frequencies of these kinds of structures [5]. Extreme wind events compete with earthquakes as the dominant environmental design loading for structures. Both loads have caused catastrophic damage over the past years, although large damaging earthquakes have tended to occur less often than severe windstorms. On almost every day of the year a severe windstorm is happening somewhere on earth. Although many storms are small and localized, the most severe of all wind events, tropical cyclone, initiates over tropical oceans, causing huge losses to life and properties.

(2) Wind Effects on Buildings. Wind can be low, moderate, strong, and extremely destructive. While low and moderate winds are beneficial for pollution dispersion and electric power generation, strong and extreme wind events can cause devastating effects on the infrastructure. Extreme winds may cause damage to low-rise buildings in a form of windows damage, roof loss, or even complete collapse of wooden structures. In tall buildings, however, both cladding loads and the dynamics of the structure become a concern. High-rise buildings are amongst the more wind-sensitive structures. The lateral wind load imposed on super tall structures is generally the governing factor in the structural design. It was inevitable that their response to wind would be of concern to structural engineers and attract the interest of early experimenters, both in the wind tunnel and in full scale. Wind loads and the associated structural responses are a governing factor in the design of the steel framing system of many high-rise buildings. Wind load capacity is also a key factor in determining the overall strength of towers. In addition, the design of high-rise buildings should take into account the comfort criteria due to the wind-induced vibration.

Wind-induced response/loading in structures depend on, among other factors, the following: (1) terrain or mean

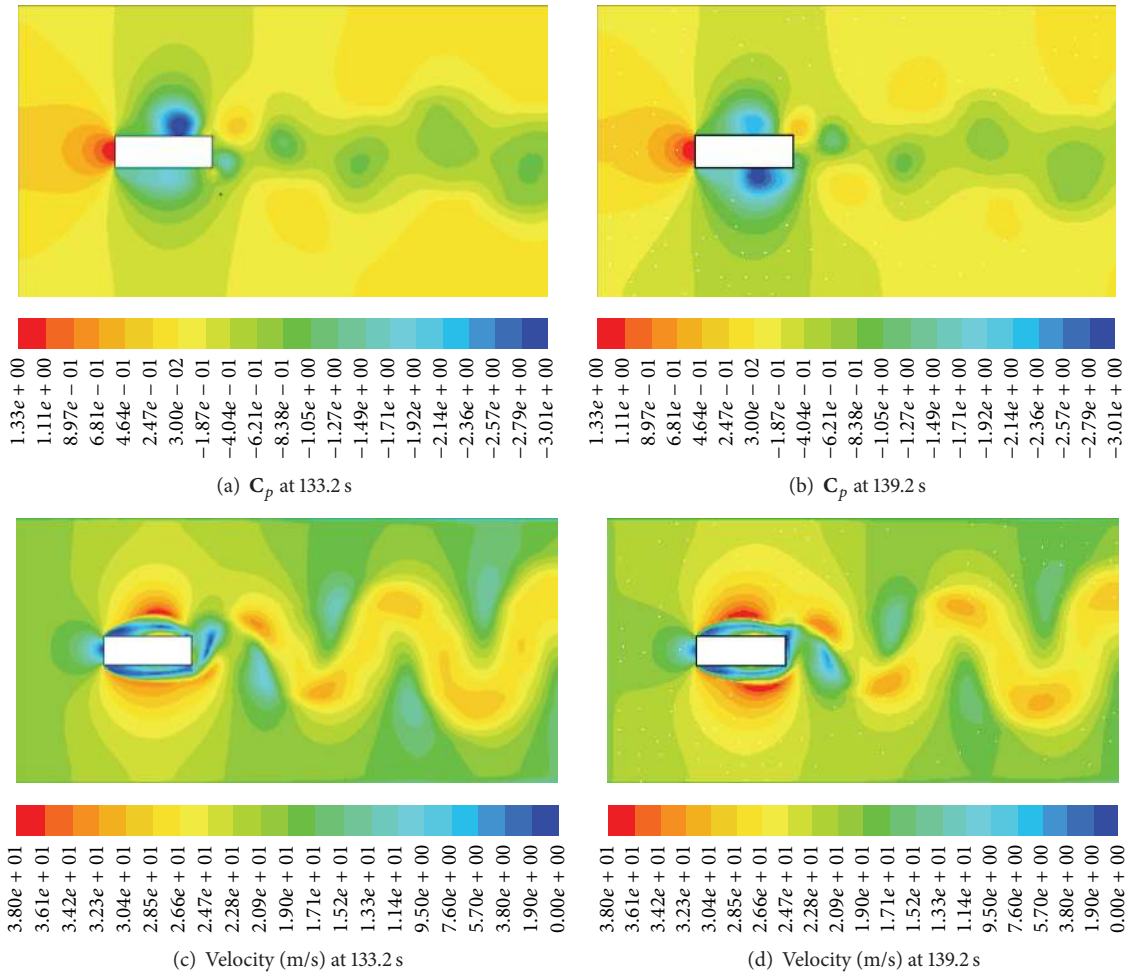

(a) $\mathbf{C}_p$ at 133.2 s

(b) $\mathbf{C}_p$ at 139.2 s

(c) Velocity (m/s) at 133.2 s

(d) Velocity (m/s) at 139.2 s

FIGURE 2: Vortex shedding phenomenon: (a) and (b) represent pressure coefficients at two time instants; (c) and (d) designate velocity contours at the same time instants.

wind velocity profile and turbulence characteristics, (2) building's aerodynamic shape (e.g., [6, 7]), (3) wind speed (which should not be always high to cause damage; when Tacoma Narrows bridge failed it was moderate wind speed but negative aerodynamic damping or self-excitation existed [8]), (4) wind direction and interference effects [9], and (5) structural properties that may magnify wind loads at resonance. Not only is the wind approaching buildings a complex phenomenon, but the flow pattern generated around buildings is complicated too. The flow pattern is distorted by the mean flow, flow separation, the formation of vortices, and development of the wake. Large wind pressure fluctuations due to these effects can occur on the surface of a building. As a result, large aerodynamic loads are imposed on the structural system and intense localized fluctuating forces act on the facade of such structures. Under the collective influence of these fluctuating forces, a building tends to vibrate in rectilinear and torsional modes [10].

Along-wind loading and response of buildings due to buffeting can be assumed to consist of a mean component due to the action of the mean wind speed (the mean hourly wind speed) and a fluctuating component. This is the basis of the so-called "gust-factor" approach, which is treated in many design codes. The mean load component is evaluated from the mean wind speed using pressure and load coefficients. The fluctuating loads are determined separately by a method which makes an allowance for the intensity of turbulence at the site, size reduction effects, and dynamic amplification [11]. The dynamic response of buildings in the along-wind direction can be predicted with reasonable accuracy by the gust factor approach, provided the wind flow is not significantly affected by the presence of neighboring tall buildings or surrounding terrain.

Crosswind oscillations can be excessive, especially if the structural damping is small. The most common source of crosswind excitation is that associated with "vortex shedding" [12, 13]. Tall buildings are bluff (as opposed to streamlined) bodies that cause the flow to separate from the surface of the structure rather than follow the body contour (Figure 2). The asymmetric pressure distribution, created by the vortices around the cross section, results in an alternating transverse force as these vortices are shed. If the structure is flexible, oscillations are transverse to the wind. The conditions for resonance would exist if the vortex shedding frequency

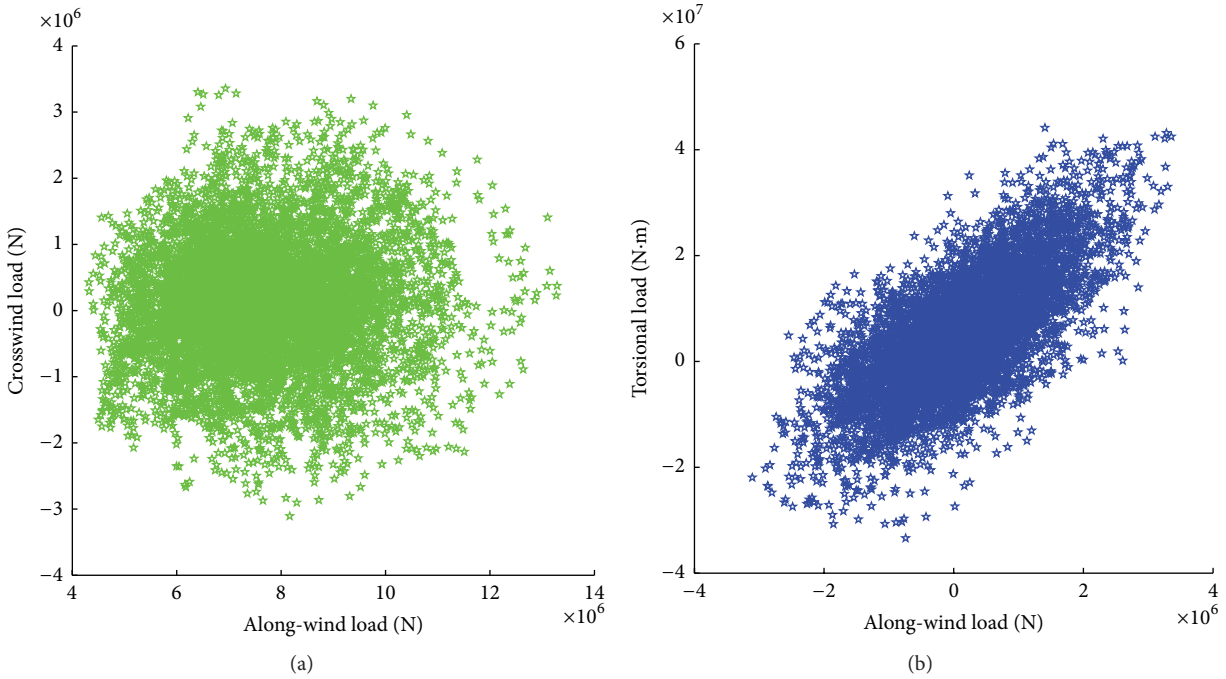

FIGURE 3: Plots among different load components for a wind direction angle of 90°: (a) overall crosswind load versus the overall along-wind load and (b) overall torsional load versus the over along-wind load.

coincides with the natural frequency of the structure. This situation can give rise to excessive oscillations and possibly failure.

Figure 3 presents plots among overall along-wind, crosswind, and torsional pressure loads obtained from wind tunnel testing of a tall building [14]. The target is to see if there are any correlations between any two of these load components. The figure shows that there is no correlation between the along-wind and the crosswind loading. There is no correlation also between the along-wind and the torsional loads. However, the crosswind and the torsional loads showed some correlations. The correlation between the crosswind and the torsional loads depends on the geometry of the building. That is, the correlation is strong at a direction angle of 90° while the two load components are less correlated at 180°, angle of attack.

Structural innovations and lightweight construction technology have reduced the stiffness, mass, and damping characteristics of modern buildings. In buildings experiencing wind motion problems, objects may vibrate, doors and chandeliers may swing, pictures may lean, and books may fall off shelves. If the building has a twisting action, its occupants may get an illusory sense that the world outside is moving, creating symptoms of vertigo and disorientation. In more violent storms, windows may break, creating safety problems for pedestrians below. Sometimes, strange and frightening noises are heard by the occupants as the wind shakes elevators, strains floors and walls, and whistles around the sides.

Wind Loading Prediction. A vital part of the design of modern tall buildings is the prediction of wind-induced motion and the assessment of its effects on occupant comfort. One of the primary purposes of wind engineering research is to predict wind-induced forces on structures. Wind-induced forces are dependent on the shape of the structure [6, 7], location on the structure, and the characteristics of wind (such as wind speed and angle of attack). Traditionally, wind loading on buildings can be evaluated analytically using some codes and formulas [15–19]. However, these standards provide little guidance for the critical crosswind and torsional loading. This is partially attributed to the fact that the crosswind and torsional responses, unlike the along-wind responses, result mainly from the aerodynamic pressure fluctuations in the separated shear layers and the wake flow fields, which have prevented, to date, any acceptable direct analytical relation to the oncoming velocity fluctuations [20]. Also, these methods have limitations, especially when other tall structures exist in the vicinity of the building under consideration. Moreover, the evaluation process depends on many assumptions. To alleviate these problems, wind tunnel testing can provide a more reliable solution.

Despite recent advancements in computational fluid dynamics, wind tunnel simulation of a scaled model is still the most common tool used to predict wind loading. Wind loads may be derived through multiple point synchronous scanning of pressures or by measuring forces on the model mounted on a high frequency force balance (HFFB). High frequency force balance (HFFB) technique has been widely recognized for conveniently quantifying generalized wind forces on tall buildings [21, 22]. The generalized forces are then utilized for estimating building response with given structural characteristics. The HFFB technique generally requires mode shape corrections which are based either on

empirical corrections or analytical formulations derived on the basis of assumed wind loading models.

The integrated pressure modal load or IPML technique has the potential of addressing all of the limitations of the conventional high-frequency force-balance technique while still maintaining the same advantages that the technique has over the aeroelastic modeling [23]. Surface pressure measurement is favorable over force balance measurement as it gives the load distribution over the building surface and it cancels out the inertial effects [24]. The pressure integration technique can also be used to examine higher modes with nonmonotonic mode shapes. The advantage of this technique is also that a single model used in a single testing session can produce both overall structural loads and cladding loads.

(3) Earthquake Effects on Buildings. In a response to the earthquake ground motion, buildings vibrate under inertia loads that may cause excessive stresses in weak walls, columns, beams, and/or joints, resulting in partial failure or even complete collapse. The type of the ground motion and the corresponding structural response vary, depending on location and the physical properties of the building (mass, stiffness, and damping). High-rise and slender structures tend to amplify the motions of longer periods when compared with short buildings. Also, taller buildings tend to shake longer than short buildings. However, tall buildings are usually built to withstand strong wind loads and precautions are taken to increase the damping, which may make them deform less under earthquakes [25].

Compared to windstorm disasters, the mortality in earthquakes is relatively high owing to the difficulty in predicting the event over a time sufficient for evacuation [26, 27], among other factors. The California quakes of 1971, San Fernando, the 1989 Loma Prieta, and the 1994 Northridge, are the 6th, 9th, and 10th most deadly events [28]. According to Vranes and Pielke Jr. [28], the 1906 San Francisco earthquake and fire which adjusts to $39–$328 billion is likely the most costly natural disaster in U.S. history in normalized 2005 values.

Earthquake Loading Prediction. Preparing buildings (either new or old) to survive strong earthquakes is expensive and the level of investment involves social and political aspects. The choice of a certain building design is a compromise among appearance, function, strength, engineering preference, type of structure, location, nature of the dynamic load, and of course project commissioning. Standards are instituted through the establishment of building codes, which regulate the design and construction of buildings (e.g., [15, 29]). These standards were written to protect first the building occupants and second the building integrity. Building codes are usually drafted to meet the demands of the expected ground motions at a certain location that are presented by hazard maps. Hazard maps are constructed by examining the following:

(i) The earthquake history of the region to estimate the probability of an earthquake.

(ii) The expected shaking intensity produced by the earthquake (often expressed as a peak acceleration).

(iii) The frequency of the shaking and the distance from the fault.

(iv) The regional geology and site conditions.

According to Koulouras et al. [30], laboratory studies show that electromagnetic emissions in a wide frequency spectrum ranging from kilohertz (kHz) to megahertz (MHz) frequencies are produced by the opening of microcracks, with the MHz radiation appearing earlier than the kHz radiation. Since earthquakes are large-scale fracture phenomena in the Earth's heterogeneous crust, the radiated kHz-MHz electromagnetic emissions are detectable at a geological scale. A technique that uses the earth's electromagnetic emissions to predict earthquakes before its occurrence by a few days to a few hours before destructive earthquakes in Greece is discussed in Koulouras et al. [30].

Although there are higher chances of constructing buildings on regions where both wind and earthquake hazard present a real threat, current design codes and hazard mitigation strategies treat hurricanes and earthquakes as completely independent, which does not account for the increased risk to structures in regions where both hazards are present [2]. Potra and Simiu [31] used a numerical method to obtain optimized design variables for sites subjected to both wind and earthquake hazards individually and simultaneously (see also [32, 33]). Li and Ellingwood [34] developed a framework for multihazard risk assessment and mitigation for wood-frame residential construction.

(4) Layout of the Paper. The current paper presents investigations on the dynamic response of a high-rise building that is instructive. The building has two different characteristics in the two lateral directions. Both wind and earthquake impacts on the responses of the building in the two directions are studied. The paper is organized as follows. Section 2 represents finite element modelling (FEM) of a high-rise building, as a case study, with modal equations of motion. In Section 3, the response of the building to wind loading is presented, by both rigid model and aeroelastic concepts. In Section 4 the response of the building to earthquake ground motion is presented, along with comparison with those obtained under wind loads, and highlights the basic differences between the two types of hazards (wind and earthquakes). In addition, Section 4 also presents the responses of another tall building (76-story building) for further comparisons. Section 5 illustrates different mitigation techniques that may be applicable for both hazards. Section 6 discusses the need for developing a decision support tool to assist decision makers in the mitigation and retrofitting of buildings for multihazard, to improve the safety and sustainability of buildings. Finally, the conclusions drawn from the current paper are presented in Section 7.

2. High-Rise Building Model (54-Story Building)

2.1. Description of the Building. The first tower considered in the current study represents a full-scale building with

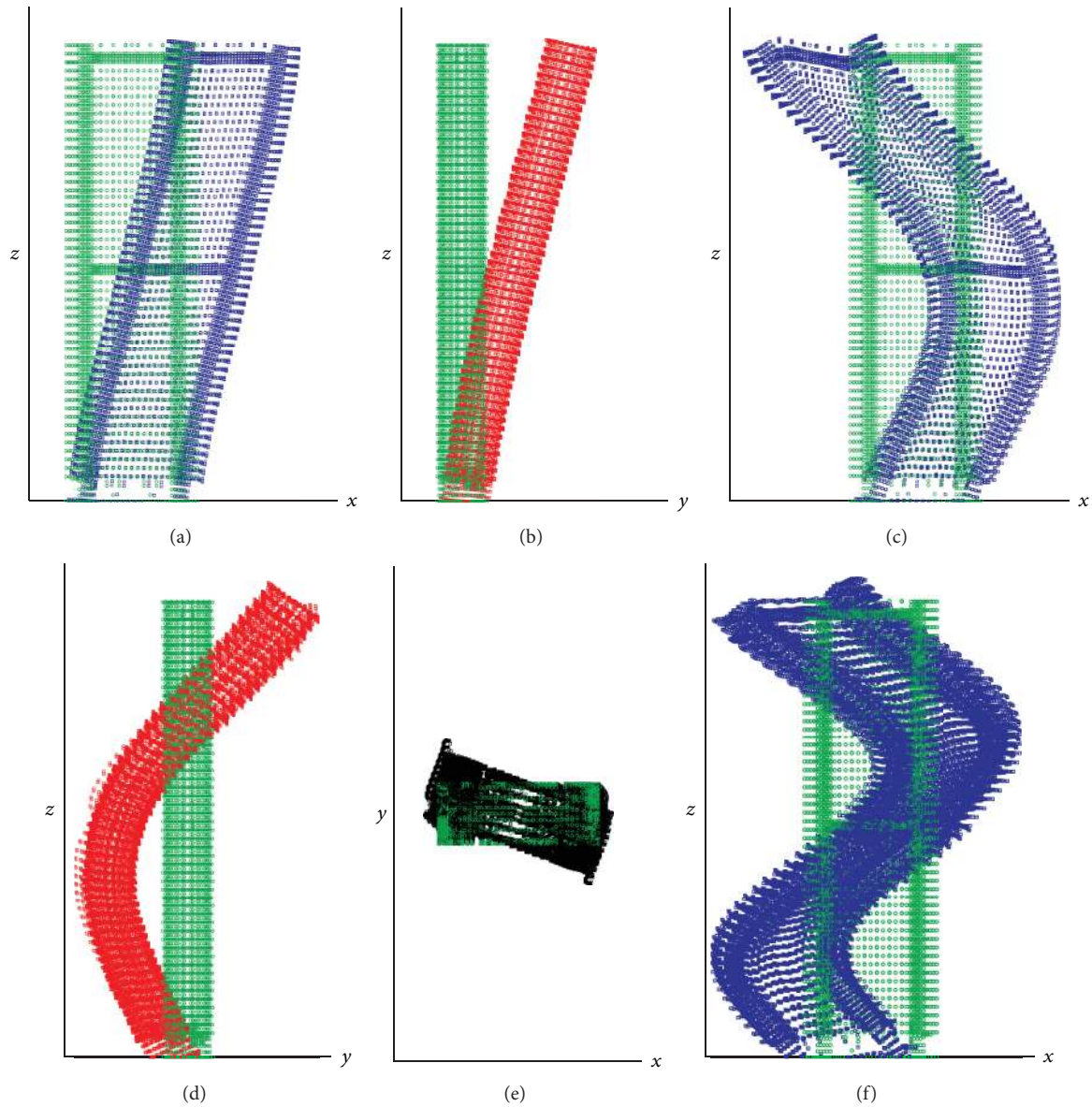

Figure 4: Mode shapes of the FEM with the coordinate system: (a) first mode in x-dir.; (b) second mode in y-dir.; (c) third mode in x-dir.; (d) fourth mode in y-dir.; (e) fifth mode about z-axis (torsion); and (f) sixth mode in x-dir. (54-story building).

a height of 221 m above ground, intended to have offices with restaurants at the top story. It has an aspect ratio of about 9.5, which makes it sensitive to strong winds. The overall building's mass is about 1.4×10^5 tons, with fifty stories above ground. The ground story has a height of 12.3 m, the successive stories have heights of 4.1 m, and the last three stories have heights of 8.4 m, 4.2 m, and 3.8 m, respectively. In addition to the fifty stories above ground, there are four underground stories: story-1 has a height of 7 m, story-2 has a height of 4 m, story-3 has a height of 5 m, and story-4 has a height of 3 m. In terms of the main force resisting system, the building has two reinforced concrete cores proposed to carry lateral loads and part of the vertical loads. However, the building has distributed vertical columns to carry the rest of the vertical load. To permit structural behavior investigation under dynamic loads, a FEM was developed (the first six mode shapes of the building are shown in Figure 4). The modal parameters of the FEM for the first six modes are given in Table 1.

Although finite element software packages can help provide mode shapes, modal masses, and modal frequencies, they do not provide information about damping in buildings. This is because, unlike mass and rigidities that are distributed in a well-known matter along structural elements, damping however is related to friction between joints and hysteresis in the material which make it difficult to be modeled [35]. However, there is no convenient mean to refine the predictive capabilities regarding inherent structural damping, owing to its association with a number of complex mechanisms and even nonstructural elements.

Table 1: Parameters of the FEM (corresponding mode shapes are shown in Figure 4).

Mode number	Direction	Generalized mass, (kg·m^2)	Frequency, (Hz)
1	Lateral in x-direction	3.55×10^7	0.1223
2	Lateral in y-direction	3.13×10^7	0.1352
3	Lateral in x-direction	3.27×10^7	0.4609
4	Lateral in y-direction	3.27×10^7	0.6473
5	Torsional	2.08×10^{10}	1.0789
6	Lateral in x-direction	4.50×10^7	1.0833

Full-scale measurements are considered the most reliable method to evaluate the dynamic characteristics of buildings and other structures. While the best way to obtain information about damping is to perform full-scale measurements, there have been some efforts to develop empirical predictive tools for damping estimation based on full-scale observations [36, 37]. According to these measured data and for a reinforced concrete (RC) building with a height of about 240 m (including underground stories), the corresponding damping factor according to the lower trend line is about 0.6%. Tamura and Yoshida [38] presented a damping predictor for tall buildings that is dependent on the amplitude. The formula for RC buildings is given by

$$\zeta = \frac{0.93}{H} + 470\frac{x_H}{H} - 0.0018, \tag{1}$$

where ζ is the first modal damping, x_H is the displacement at the top of the building, and H is the building's height. For $x_H = 0.5$ m and overall building height of about 240 m the damping factor from (1) is about 1%. For $x_H = 0.25$ m and 1 m the corresponding damping factors are 0.5% and 2%, respectively. However, the damping factor for the building was assumed to be 1%.

2.2. Equation of Motion. The generic equations of motion governing the behavior of the building under wind loads may be written as

$$\mathbf{M}\ddot{\mathbf{X}} + \mathbf{C}\dot{\mathbf{X}} + \mathbf{K}\mathbf{X} = \mathbf{F}(t), \tag{2}$$

where $\mathbf{X} = [\mathbf{x}\ \mathbf{y}\ \mathbf{z}]^T$ is a $3n \times 1$ vector and n is the number of nodes while $\mathbf{x}$, $\mathbf{y}$, and $\mathbf{z}$ are vectors of nodal displacement in x-, y-, and z-directions, respectively. $\mathbf{F}(t) = [\mathbf{F}_x(t)\ \mathbf{F}_y(t)\ \mathbf{F}_z(t)]^T$, in which $\mathbf{F}_x(t)$, $\mathbf{F}_y(t)$, and $\mathbf{F}_z(t)$ are $n \times 1$ vectors of external forces acting in x-, y-, and z-directions, respectively. Using the first six modes obtained by FEM, it was shown that there is no significant increase in the wind-induced responses if modes higher than the sixth mode are considered for this specific structure, with the next transformation

$$\mathbf{X} = \mathbf{\Phi}\mathbf{Q}, \tag{3}$$

where $\mathbf{\Phi}$ is $3n \times 6$ matrix of eigenvectors and $\mathbf{Q}$ is 6×1 vector of generalized displacement. Substituting (3) into (2) and premultiplying by $\mathbf{\Phi}^T$, one obtains

$$\mathbf{\Phi}^T\mathbf{M}\mathbf{\Phi}\ddot{\mathbf{Q}} + \mathbf{\Phi}^T\mathbf{C}\mathbf{\Phi}\dot{\mathbf{Q}} + \mathbf{\Phi}^T\mathbf{K}\mathbf{\Phi}\mathbf{Q} = \mathbf{\Phi}^T\mathbf{F}(t). \tag{4}$$

By assuming the damping matrix, $\mathbf{C}$, to be proportional damping, (4) results in six uncoupled equations

$$\begin{aligned}
m_{11}\ddot{q}_1 + c_{11}\dot{q}_1 + k_{11}q_1 &= \sum_{i=1}^{n}\phi_1(x_i)F_{x,i}(t) \\
&+ \sum_{i=1}^{n}\phi_1(y_i)F_{y,i}(t) + \sum_{i=1}^{n}\phi_1(z_i)F_{z,i}(t) = GF_1, \\
m_{22}\ddot{q}_2 + c_{22}\dot{q}_2 + k_{22}q_2 &= \sum_{i=1}^{n}\phi_2(x_i)F_{x,i}(t) \\
&+ \sum_{i=1}^{n}\phi_2(y_i)F_{y,i}(t) + \sum_{i=1}^{n}\phi_2(z_i)F_{z,i}(t) = GF_2, \\
&\vdots \\
m_{66}\ddot{q}_6 + c_{66}\dot{q}_6 + k_{66}q_6 &= \sum_{i=1}^{n}\phi_6(x_i)F_{x,i}(t) \\
&+ \sum_{i=1}^{n}\phi_6(y_i)F_{y,i}(t) + \sum_{i=1}^{n}\phi_6(z_i)F_{z,i}(t) = GF_6,
\end{aligned} \tag{5}$$

where m_{ii}, c_{ii}, k_{ii}, and GF_i are generalized mass, generalized damping coefficient, generalized stiffness coefficient, and generalized force of the ith mode, respectively. The $\mathbf{q}_i(t)$ are then solved from each of the above equations. A SIMULINK model was developed to permit the numerical solution of these equations in MATLAB [39].

3. Response under Wind Loading (54-Story Building)

To obtain the wind-induced responses of the tower, the wind load time history from a wind tunnel experiment was used [14, 24]. The finite element described within the previous section allowed the evaluation of the dynamic response using the pressure integration technique [23, 40]. Two important voids associated with procedures to aid in the response prediction are considered: the first is on the distributions of the wind loads and the second is on the effects of the mode shapes. These two issues are fully addressed by using wind tunnel test data of intensively distributed pressure taps on the outer surfaces of the building, which was then integrated with the FEM. The tower responses in the two lateral directions combined with the torsional responses (effect of higher modes on the responses is studied) are obtained using the abovementioned modelling. First, the generalized forces for each mode were obtained. Second, the equations of motion in the modal form were integrated numerically. Finally the obtained responses were presented along with comparisons with most common design standards. The procedure is summarized as follows.

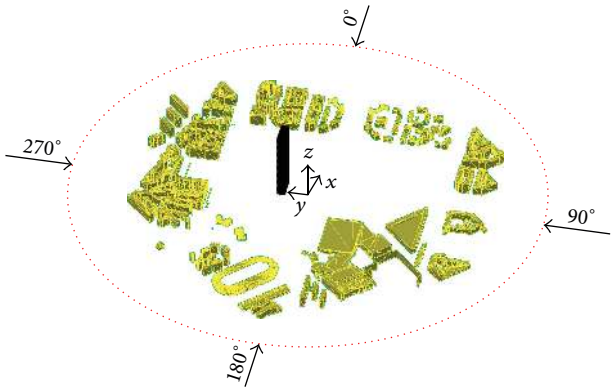

Figure 5: Original orientations of the building with its surrounding.

3.1. Generalized Forces. Using the measurements obtained by the pressure transducers, pressure coefficients (matrix $\mathbf{C}_p$) are evaluated at each tap as a function of both space and time [14, 23]. These values are to be used with the full-scale model to provide the pressure distribution on the surface for different wind direction angles (Figure 5). The pressure values on the surface of the full-scale building model can be expressed as follows:

$$\mathbf{P} = \frac{1}{2}\rho U^2 \mathbf{C}_p \left(\text{space}, \text{time}\right), \tag{6}$$

where $\mathbf{P}$ is a matrix containing the pressure values on the surface of the full-scale model as a function of space (x, y, and z) and time, ρ is the air density which is assumed to be 1.25 kg/m^3 (according to [16]), and U is the mean wind speed that is dependent of the wind directional angle (directionality effects were considered) and the period of return.

The wind load at each node of the outer surface is the integration of the pressure over the surface area in the vicinity of the node as follows:

$$\mathbf{F} = \int \mathbf{P}\left(\text{space}, \text{time}\right) dA. \tag{7}$$

The tributary areas for pressure taps and the surface FEM nodes were calculated in a computerized approach as proposed in Aly [40]. Once the time history of the pressures on the outer surfaces is calculated, the external forces acting on the nodes of the surface can be computed. The excitation forces acting on the internal nodes are of course equal to zero. Accordingly, the generalized forces are obtained as follows:

$$\mathbf{GF} = \Phi^T \mathbf{F}. \tag{8}$$

Figures 6 and 7 show the time history and the Fast Fourier Transform (FFT) of the generalized forces for the first two modes under a wind direction angle of 90° and a return period of 10 years. The maximum values of the generalized forces are obtained as expected with the second mode. This is because the second mode of the building is a lateral vibration that coincides with the direction of the applied wind (the along-wind loads are higher than the crosswind loads for this specific angle due to the bigger drag surface). It is shown in the figure that the FFT of the generalized force of the second mode indicates that the forces with high amplitudes occur at lower frequencies than that of the first mode. This means that, unlike the along-wind loads, crosswind excitations occur at relatively higher frequencies, which means that the crosswind fluctuating response may be higher than the along-wind response.

Table 2: Displacement of the top corner of the building (for wind direction angle of 90°).

Modes	RMS disp., m		Mean disp., m		Peak disp., m	
	x	y	x	y	x	y
1	0.063	0.0024	0.009	0.000	0.246	0.009
1 : 2	0.063	0.074	0.003	0.157	0.242	0.409
1 : 3	0.063	0.074	0.003	0.157	0.243	0.409
1 : 4	0.063	0.074	0.003	0.155	0.243	0.405
1 : 5	0.063	0.074	0.003	0.155	0.243	0.405
1 : 6	0.063	0.074	0.003	0.155	0.243	0.405

Table 3: Acceleration of the top corner of the building (for wind direction angle of 90°).

Modes	STD acceleration [milli-g]		Peak acceleration [milli-g]	
	x	y	x	y
1	3.49	0.13	14.41	0.54
1 : 2	3.49	4.89	14.33	18.71
1 : 3	3.53	4.89	14.97	18.71
1 : 4	3.53	4.93	14.97	20.80
1 : 5	3.54	4.94	15.01	21.03
1 : 6	3.54	4.94	15.85	21.10

Note: 1 milli-g is about 0.01 m/s^2.

3.2. Response under Wind. Once the generalized forces are obtained from (8), (5) are numerically solved to provide the generalized displacement, and then from (3) the real responses are obtained (i.e., using the pressure integration technique [23]). Table 2 lists the response of the tower in the along-wind (y-direction) and the crosswind (x-direction) directions for a wind direction angle of 90° with different considerations of the number of modes. It is shown that the displacement response of the building is dominated by the first two vibrational modes. However, the acceleration response is contributed not only by the first two lateral vibrational modes but also by higher modes (Table 3). As listed in Table 3, by considering only the first mode, the peak acceleration in the x-direction is 14.41 milli-g, and by taking into account the first six modes, the peak acceleration is increased to 15.85 (9% increase). Similarly in the y-direction, the increase from considering only the first and the second modes to account for the first six modes is 11%.

FFT of the displacement and acceleration responses of the top corner of the building are shown in Figures 8 and 9. Similar to the results in Table 3, it is shown that the acceleration response is contributed not only by lower frequencies but also by higher frequencies (higher modes),

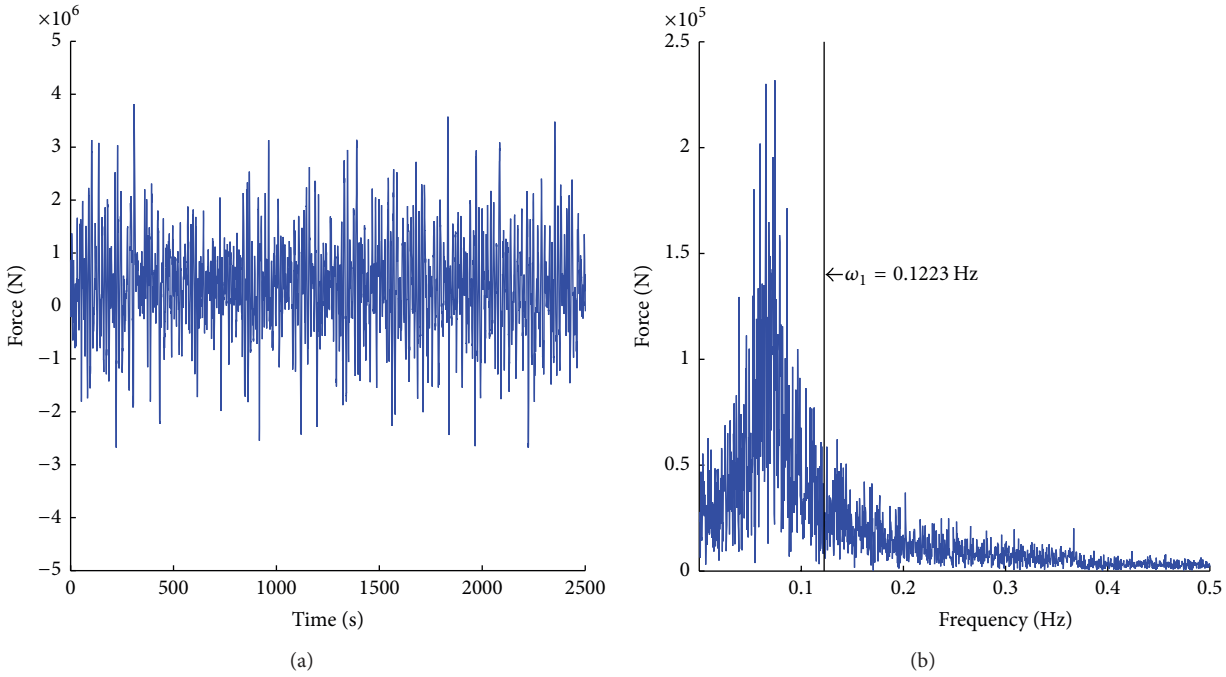

Figure 6: First mode generalized force for a wind direction angle of 90°: (a) time history and (b) FFT. Note that this mode is in the crosswind direction and the gap between peak loads and the dominant frequency (ω_1) is less than that with the second mode (ω_2 in Figure 7) (54-story building).

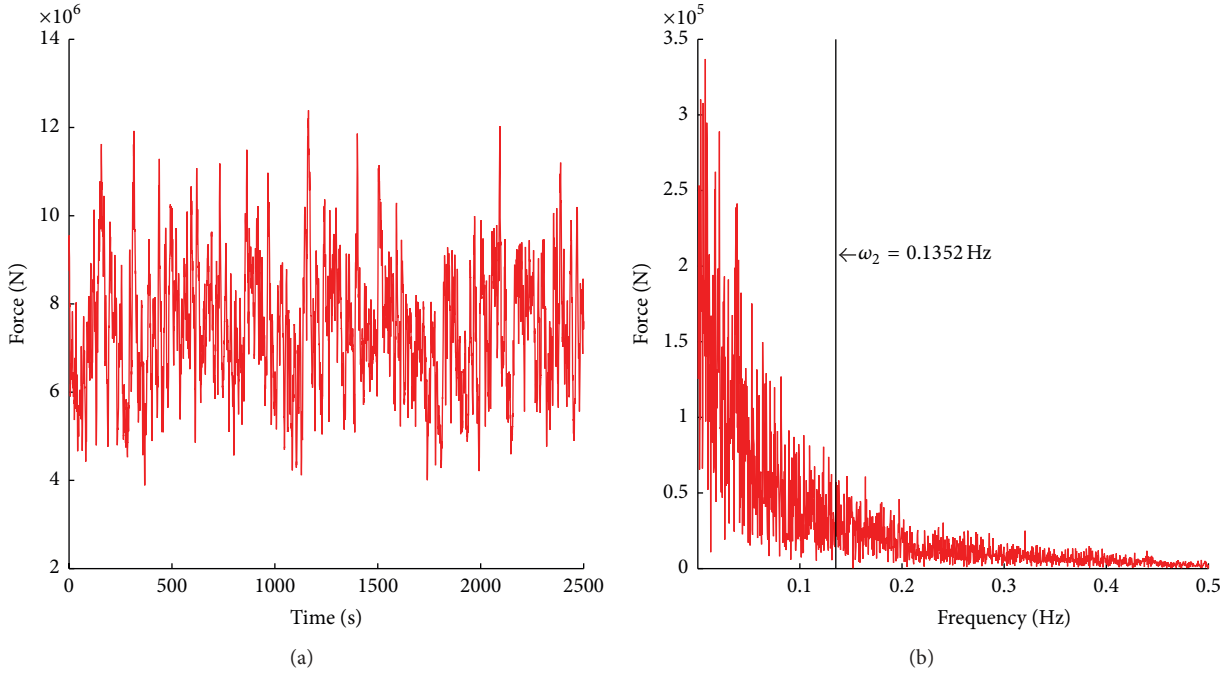

Figure 7: Second mode generalized force for a wind direction angle of 90°: (a) time history and (b) FFT. Note that this mode is now in the along-wind direction (54-story building).

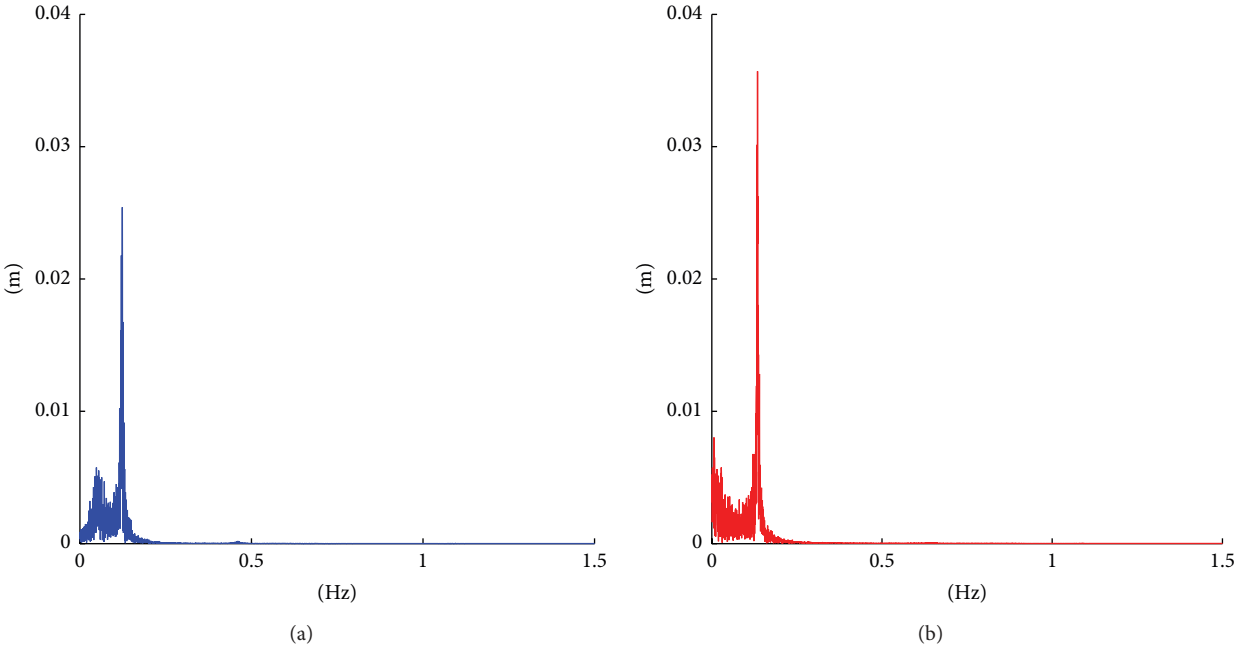

FIGURE 8: Frequency content of the displacement response of the top corner of the building for a wind direction angle of 90° (54-story building).

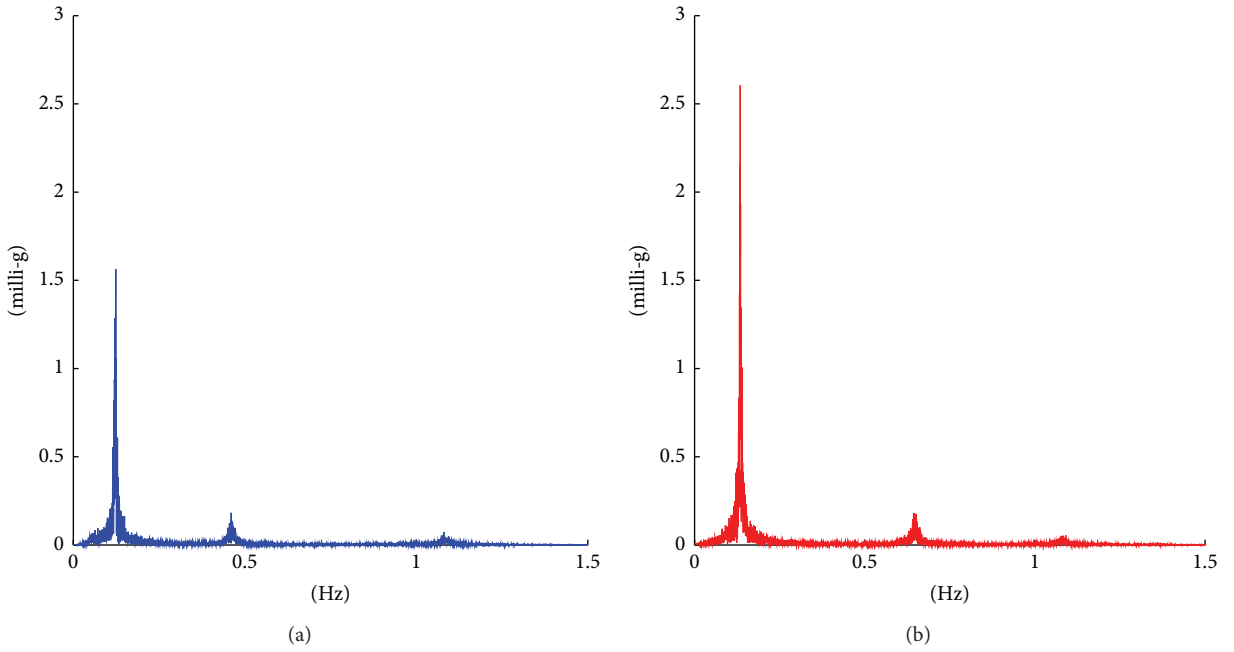

FIGURE 9: Frequency content of the acceleration response of the top corner of the building for a wind direction angle of 90° (54-story building).

while the displacement is dominantly contributed by lower frequencies (lower modes).

3.3. Comparison with Codes. The American and the European standards [15, 16] are used to obtain the along-wind responses of the tower, approximated by a rectangular prism in its outer shape. For the American standard [15], the basic wind speed is defined over a period of 3 seconds. To obtain the basic wind speed over a period of 3 seconds it is necessary to find the mean hourly wind speed. The mean hourly wind speed is obtained using the formula ([41, eq. (2.3.37)] of the book)

$$U_t(z) = U_{3600}(z)\left(1 + \frac{\beta^{1/2} c(t)}{2.5 \ln(z/z_0)}\right). \quad (9)$$

Table 4: Comparisons of the along-wind responses with codes.

Results	ASCE	Eurocode	FEM
STD displacement [m]	—	0.094	0.074
Peak displacement [m]	0.375	0.428	0.405
STD acceleration [milli-g]	4.90	7.67	4.94
Peak acceleration [milli-g]	18.02	24.25	21.10

The procedure followed to obtain the response of the building using the Eurocode is further explained in Aly [23].

Table 4 gives the along-wind displacement and acceleration responses obtained using ASCE 7-2010, Eurocode 1, and the proposed method (FEM) under wind direction angle of 90°. It is shown that there are reasonable agreements among the results obtained using the two standards and the procedure followed in the current study. However, the numerical technique used has the following advantages:

(i) It combines simultaneously the responses in the along- and crosswind directions with torsion.

(ii) Higher modes can be considered (higher modes are shown to be important especially for the acceleration response).

(iii) The maximum values of the responses may occur at angles other than 0° and 90° (the wind direction angle cannot be easily considered by using a design standard).

(iv) The responses in the crosswind direction may be larger than those in the along-wind direction. This reveals the importance of the technique proposed as many standards provide details to calculate the along-wind response but not the critical crosswind and torsional responses.

The comfort criterion for this building is that the peak acceleration should not exceed 20 milli-g under wind with a return of 10 years. This means that if an acceleration peak factor of 3.5 is used, the RMS acceleration should not exceed 5.7 milli-g.

3.4. Effects of the Wind Direction Angle and the Orientation on the Responses. Due to the fact that the mean wind velocity is unequal from all directions and the effect of the wind attack angle is important (e.g., along- and crosswind responses are not the same), one may consider rotating the building (orientation change). This may be possible if the building is still in its preliminary design stages. Since the building case study is shown to be more sensitive to crosswind loads in the y-direction, the response of the building under wind that has the same mean speed (28.5 m/s) for all the direction angles is first evaluated (Figure 10).

From Figure 10, one can see that the responses of the tower are the worst in the crosswind of the y-direction (angle 180°). A potential solution to such problem is to consider the effect of the real wind directionality (Figure 11) on the response of the tower. The results show that if the tower orientation is changed to be rotated clockwise, as shown in Figure 12 (suggested orientation), the highest response in y-direction can be dramatically reduced. This is confirmed by Figure 13. Among different possible orientations, the best orientation is shown to be the one in which the building is rotated 67.5°. Although this suggested orientation is favorable in reducing the responses in the y-direction, the response in the x-direction is slightly increased. However, the increased response in the x-direction (suggested orientation) is lower than the worst response in the y-direction (original orientation). The reduction in the worst peak acceleration over the two directions (x- and y-directions) is shown to be more than 38.5% (Figure 13). This reduction is achieved without adding any structural elements/components to the primary building (no additional cost). This confirms the advantage of rotating the building to the suggested orientation and also reveals the

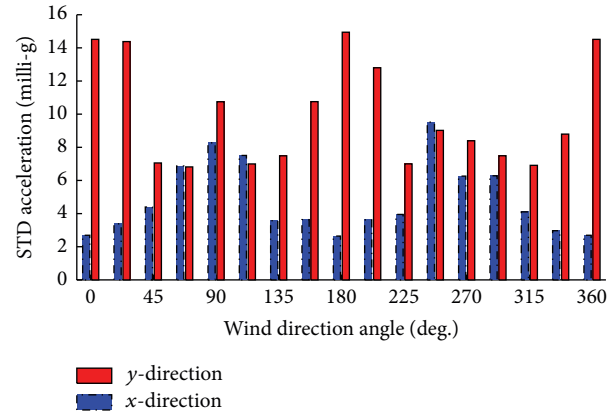

Figure 10: STD acceleration under wind velocity with same mean values (28.5 m/s) from all wind direction angles (54-story building).

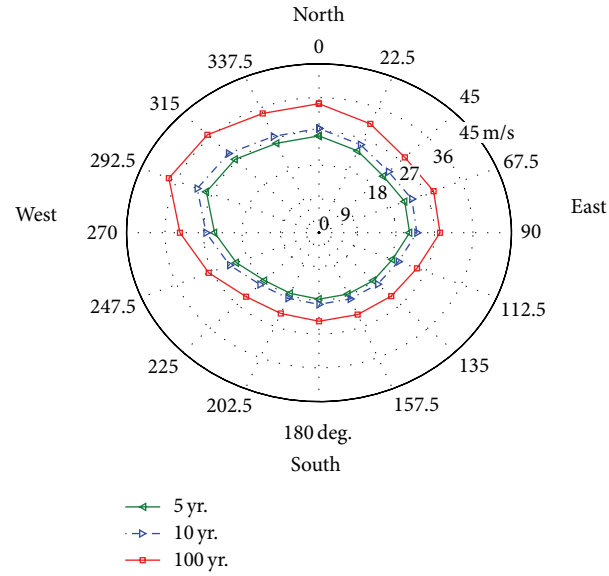

Figure 11: Wind speed directionality for three return periods: 5, 10, and 100 years. Note that the 5- and 10-year returns were used for comfort concerns; and the 100 years of return was used for the response estimation for the design aspects.

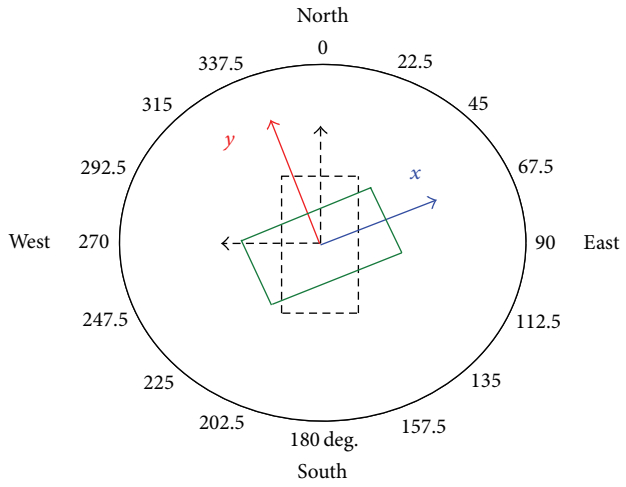

FIGURE 12: Original (dotted lines) and suggested (solid lines, rotated 67.5 deg. c.w.) orientations.

importance of the response prediction in high-rise buildings during their preliminary design stages.

3.5. Aeroelastic Response. In the previous subsections, the responses of the building were obtained numerically using wind tunnel data from a rigid model testing and FEM. Although this method is shown to be reasonable and has general agreements with recent typical standards, the method does not account for the aerodynamic damping, which can be only obtained by considering the interaction between the flow and the moving building. Such flow-structure interaction requires the aeroelastic model experiment. This subsection provides an answer to an important question; that is, is the aeroelastic model experiment necessary for such type of building? Keep in mind such experiment with its preparation can be substantially time and resource consuming. Accordingly, the same rigid model was elastically supported (see Figure 14) and its mass was adjusted [14, 42]. Beside the geometrical similarity (between model and prototype), the aeroelastic model requires the following similarities [43]:

$$\text{Mass: } \lambda_M = \lambda_L^3 \lambda_{\rho_s}, \tag{10}$$

$$\text{Velocity: } \lambda_V = \frac{U_m}{U_p}, \tag{11}$$

$$\text{Frequency: } \lambda_f = \frac{\lambda_V}{\lambda_L}, \tag{12}$$

$$\text{Damping: } \zeta_m = \zeta_p. \tag{13}$$

For a length scale λ_L of 1 : 100 and the density scale, $\lambda_{\rho s}$, of 1, the mass scale λ_M is $1 : 10^6$. Assuming the velocity scale λ_V defined in (11) to be 1 : 10, the frequency scale λ_f defined by (12) is 10 : 1. The steel bars at the base of the model (flexible support) were preliminary designed to give the required natural frequencies in the two lateral directions; then the distances between the bars ($\mathbf{L_x}$ and $\mathbf{L_y}$ on Figure 14) were adjusted to give the required natural frequencies experimentally. A FFT analyser was used to check the natural frequencies online. From the similarity conditions, steel bars and blocks were attached to the inside of the test model to adjust the generalized masses to be 35.5 kg·m^2 and 31.3 kg·m^2 in the x- and y-directions, respectively. The aeroelastic model had two frequencies of 1.22 Hz and 1.35 Hz in the x- and y-directions, respectively. According to (13), the damping factor of the model was set to be the same as the presumed prototype value, that is, 1% in the two lateral directions. Additional Airpots (dampers) were installed at the base of the model to adjust the modal damping (see Figure 14). The overall damping of the model was calculated from the time decay of the response using the logarithmic decrement technique. The damping of the Airpots has been changed up and down until the required amount of damping to the model was achieved. Three accelerometers were attached near the top of the building model, at a height of 1.87 m from its base. One accelerometer was used in the x-direction (with a measuring range of ±3 g), and two accelerometers were used in the y-direction (with a measuring range of ±20 g). The data of the accelerometers were acquired at a rate of 1000 Hz. An online FFT Analyser was used for direct monitoring of the measured data and to monitor the possible frequency change of the model during the test due to fluid-structure interaction. Such phenomenon occurred and a coupling between the two modes was shown at a relatively high mean wind speed (about 8 m/s, which corresponds to a prototype mean wind speed of 80 m/s). However, such wind speed is out of the predicted range of mean wind speeds at the construction site.

Since the building considered in the study has sharp-edged geometry, the results of the aeroelastic testing can be readily transformed to full-scale without concerns about Reynolds number [43]. The acceleration measurements are directly representative of the prototype response as the acceleration scale λ_A is 1 : 1. The acceleration measurements were filtered. The cut-off frequency used with the acceleration measurements was set to 10 Hz. This frequency is much more than five times the frequency of interest. Figure 15 shows the acceleration response of the building under a prototype mean wind speed of about 38 m/s. The figure provides a comparison with the response obtained by the pressure integration technique. One can see that there is a general agreement in the trend of the two methods. However the results cannot be precisely the same for the following reasons:

(i) The wind flow presents a random phenomenon and it is difficult or even impossible to have the same results for the same test under the same configurations even if it is repeated several times.

(ii) The damping produced by the Airpots (small precise pneumatic shock absorbers) and the structural part of the test model is nonlinear and may increase with the amplitude of oscillation.

(iii) The contribution of the aerodynamic damping may be positive or negative. However, the effect of the aerodynamic damping on the worst responses of the tower is shown to be positive, which resulted in partial response reduction.

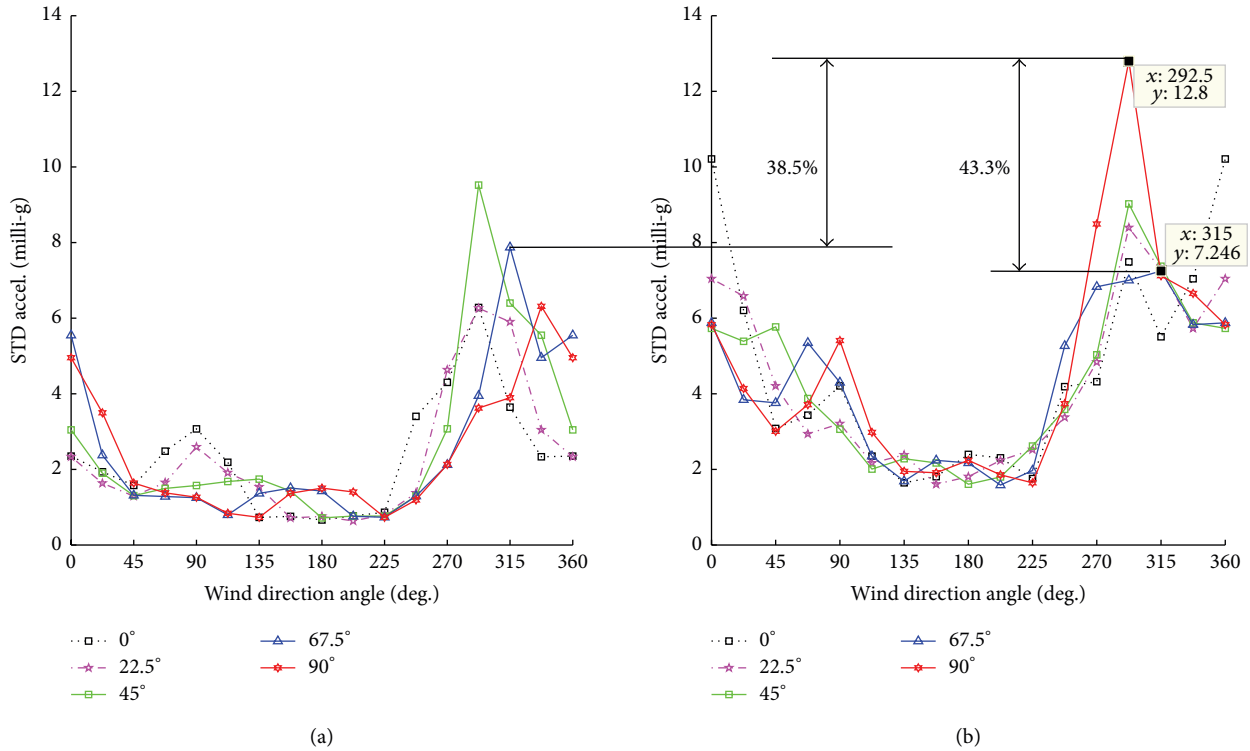

FIGURE 13: Effect of orientation change (original (0°), rotated 22.5° (c.w.), 45°, 67.5°, and 90°) on the building's response (54-story building; 5-year return period): (a) acceleration response in the x-direction and (b) acceleration response in the y-direction. Percentages of reduction are indicated in the figure.

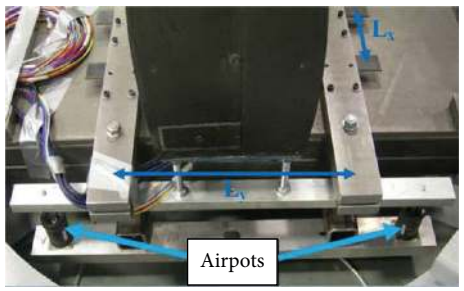

FIGURE 14: Elastically supported building model tested in a wind tunnel [14, 42].

(iv) The aeroelastic model used is simple, which represents the behaviour of a single-degree-of-freedom system in each lateral direction, while the FEM considers the contributions of higher modes.

(v) The mode shapes of the test model are of course linear while those of the FEM have a second-order trend.

Since it was noticed for this building that there is a possibility of galloping under low-turbulence flow [24], for a wind attack angle of 0°, the aeroelastic experiment was conducted to verify the existence of this phenomenon. The aeroelastic instability occurred at a model mean wind speed of 1.94 m/s (19.4 m/s prototype) and a structural damping of 0.6%. However, the galloping instability completely disappeared with higher damping (1%). Such conclusion should be taken into account for the design of similar structures in environments where low-turbulence flow is expected.

General agreement between the results of the pressure integration technique and the aeroelastic experiment is shown. Keeping in mind the complexity and the time required to prepare the aeroelastic model (especially if the model is constructed to include higher modes with exact mode shapes) and to run the experiment (more expensive), the pressure integration technique with FEM is recommended for these types of high-rise buildings. An advantage of the pressure integration technique is also that a single model used in a single testing session can produce both overall structural loads and cladding loads.

4. Response under Earthquake Loading (54- and 76-Story Buildings)

Although strong earthquakes are shown to have significant impact on short- and medium-rise buildings [44–46], their effects on super high-rise buildings can be different. To evaluate the effects of the earthquake loading on the case study building, the time history of the ground motion was first synthesized according to the applicable design standard [47], which defines the spectrum of the ground acceleration as a function of both the terrain characteristics and the typical stratigraphic profile of the site. The earthquake associated with the worst terrain type was synthesized. The spectrum of

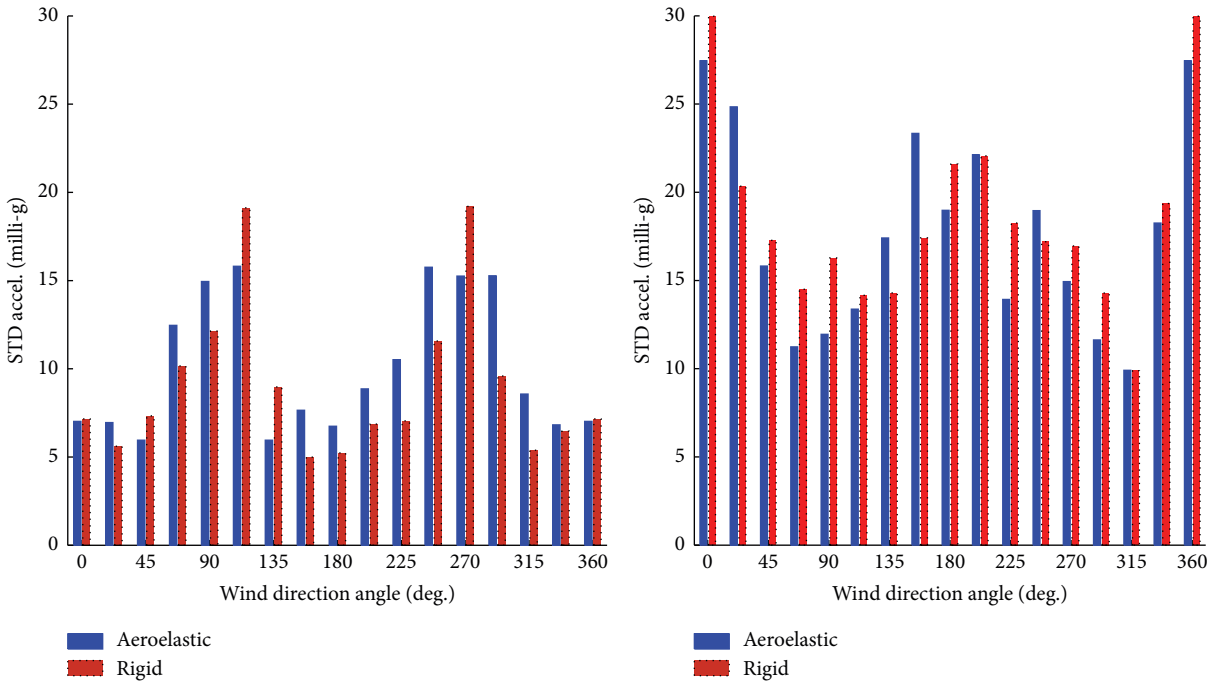

FIGURE 15: Comparisons between responses for rigid and aeroelastic models (54-story building): (a) acceleration response in the x-direction and (b) acceleration response in the y-direction. Note that these responses were obtained for a prototype wind speed of 38 m/s, uniform from all directions, and do not correspond to design for comfort and serviceability (just for the sake of comparison between the two techniques of modelling).

the ground acceleration and the corresponding time history of the ground motion are shown in Figure 16.

Since earthquakes excite higher modes more than wind loads, a lumped masses model is derived from the original FEM (54-story building). In this model, the mass of the building is lumped at the positions of floors. In general, equations of motion for an n-story building moving in both the two transverse directions may be written as follows:

$$\mathbf{M}_s\ddot{\mathbf{x}} + \mathbf{C}_s\dot{\mathbf{x}} + \mathbf{K}_s\mathbf{x} = -\mathbf{M}_s\ddot{\mathbf{x}}_g, \tag{14}$$

where $\mathbf{x} = [\mathbf{X}\ \mathbf{Y}]^T$. The terms $\mathbf{X} = [x_1\ x_2\ \cdots\ x_n]$ and $\mathbf{Y} = [y_1\ y_2\ \cdots\ y_n]$ are row vectors of the displacement of the center of mass of each floor in the x- and y-directions, respectively, while n is the number of stories. $\mathbf{M}_s$, $\mathbf{K}_s$, and $\mathbf{C}_s$ are mass, stiffness, and damping matrices, respectively, and $\ddot{\mathbf{x}}_g$ is the ground acceleration. The mass matrix $\mathbf{M}_s$ has the following form:

$$\mathbf{M}_s = \begin{bmatrix} \mathbf{M} & 0 \\ 0 & \mathbf{M} \end{bmatrix}, \tag{15}$$

where $\mathbf{M} = \text{diag}([m_1\ m_2\ \cdots\ m_N])$ is the diagonal $N \times N$ matrix of masses of each floor. N = the total number of floors. The stiffness matrix $\mathbf{K}_s$ is obtained by assuming the stiffness between adjacent floors as a combination of cantilever and shear rigidities. MATLAB [39] codes were written to derive the best stiffness matrix that provides the closest mode shapes to those of the FEM and almost the same first six natural frequencies. The stiffness matrix $\mathbf{K}_s$ has the form

$$\mathbf{K}_s = \begin{bmatrix} \mathbf{K}_x & 0 \\ 0 & \mathbf{K}_y \end{bmatrix}, \tag{16}$$

where $\mathbf{K}_x$ and $\mathbf{K}_y$ are the stiffness matrices in the transverse directions, x and y, respectively.

The most effective way to treat damping within a modal analysis framework is to consider the damping value as an equivalent Rayleigh Damping in the form of [48]

$$\mathbf{C}_s = \alpha\mathbf{M}_s + \beta\mathbf{K}_s \tag{17}$$

in which $\mathbf{C}_s$ is the damping matrix; α and β are predefined constants. After calculating the damping matrix, the modal damping vector is estimated for all the vibrational modes and the first six modal damping ratios are replaced by 1%. The damping matrix is reconstructed using the new modal damping vector. To obtain the damping matrix, $\mathbf{C}_s$ is derived using modal damping factors [49]; at normal modes (when the equations of motion are decoupled) the equations of motion for free damped vibration take the form

$$\mathbf{M}_s\ddot{\mathbf{x}} + \mathbf{C}_D\dot{\mathbf{x}} + \mathbf{K}_s\mathbf{x} = \mathbf{0}, \tag{18}$$

where

$$\mathbf{C}_D = [uu]^T [\mathbf{C}_s] [uu] = 2\mathbf{M}_s [\omega] [\zeta] \tag{19}$$

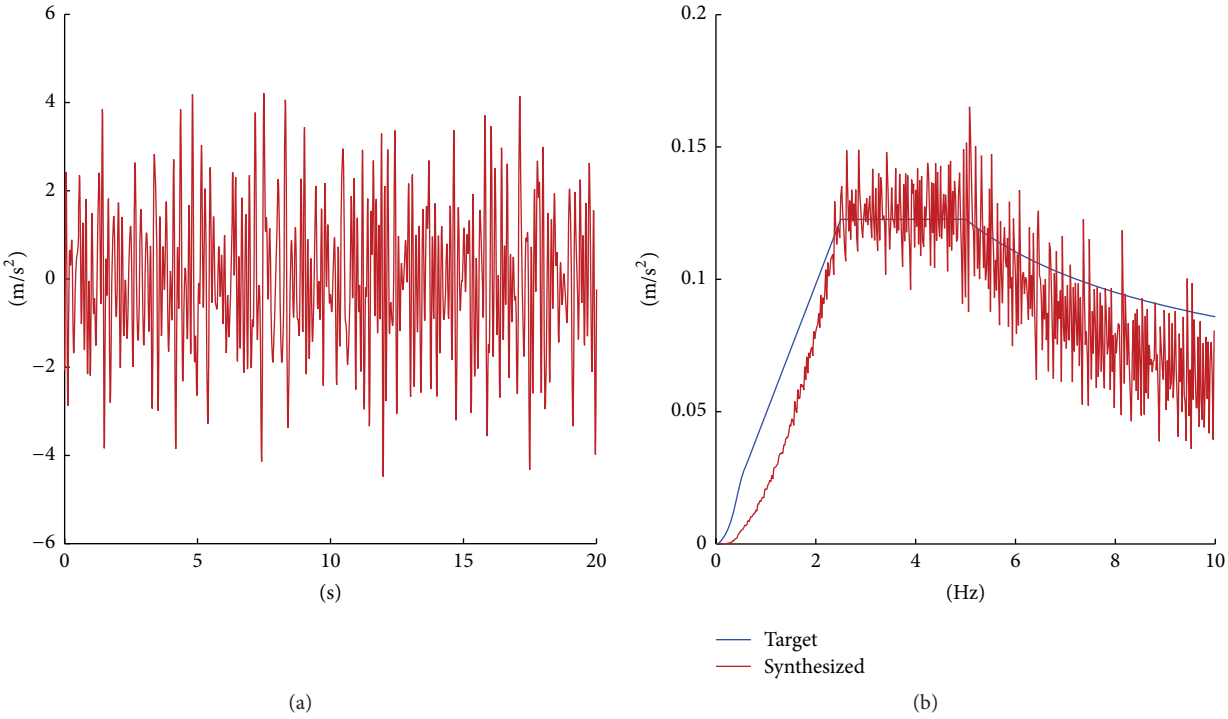

Figure 16: Ground acceleration: (a) time history and (b) spectra of target and synthesized motions.

in which $[uu]$ is the matrix of orthonormal modes associated with the eigenvalue problem (eigenvectors), $[\omega]$ is the diagonal matrix of undamped natural frequencies, and $[\zeta]$ is a diagonal matrix of modal damping.

Figure 17 gives responses of the tower due to the earthquake ground motion, along with the worst wind-induced responses in the two lateral directions. Note that, for the responses under wind, the wind speed corresponding to a return period of 100 years was used for displacement and drift evaluations; and the wind speed corresponding to a return period of 10 years was used for acceleration estimation. The interstory drift angle is defined by

$$\text{Drift angle} = \frac{x_N - x_{N-1}}{\Delta H_N}, \tag{20}$$

where x_N and x_{N-1} are the displacement of two successive floors and ΔH_N is the height of the story number N. The horizontal component of the ground acceleration is assumed to attack the building in each of the two lateral directions independently. Although the peak displacement under wind loads is much higher compared to that under the earthquake loads, the opposite is true with the acceleration response. It is shown that the interstory drift of the tower due to the earthquake loads is lower than the design value of 0.005. The figure shows that the drift response of the tower under wind loads is significantly higher than the drift under the earthquake loads for the two lateral directions. The figure also shows that the wind-induced drift in the y-direction is higher than a typical recommended design limit of 0.005. The results indicate that earthquake loads excite higher modes that produce less interstory drift but higher acceleration which occurs for short time (compared to wind loads). Although the acceleration under wind loads is lower than that under earthquake loads, it occurs for longer periods which becomes a comfort issue. However, the drift under wind is larger which raises security issues. The results also show that tall buildings designed for wind may be safe under moderate earthquake loads. It is important to mention that, even if the interstory drift ratios in tall buildings may be relatively small with no significant apparent issues for the main force resisting system of the structure, nonstructural systems may represent a high percentage of loss exposure of buildings to earthquakes due to high floor acceleration. Accordingly, appropriate damping techniques are recommended for response reduction under wind and earthquake loads.

For further comparison and validation of the conclusions obtained above, a 76-story building was studied under wind and earthquake loads. The benchmark building is defined in Yang et al. [50, 51] and Kim and Adeli [52]. Only one lateral direction was considered for response analysis under both crosswind loads and earthquakes (not simultaneously). The first three natural frequencies of the 76-story building in the lateral direction considered herein are 0.16, 0.765, and 1.992 Hz. The aspect ratio is about 7.3 and the total mass of this building is 153,000 tons. Similar to the conclusions obtained with the 54-story building, Figure 18 shows that the wind loads produce significant drift and displacement, compared to the earthquake loads. Again the acceleration responses under the earthquake motion are extremely high compared to those under wind loads. Even though the acceleration response under wind loads (about 30 milli-g at floor 75) still represents comfort and serviceability issues, the

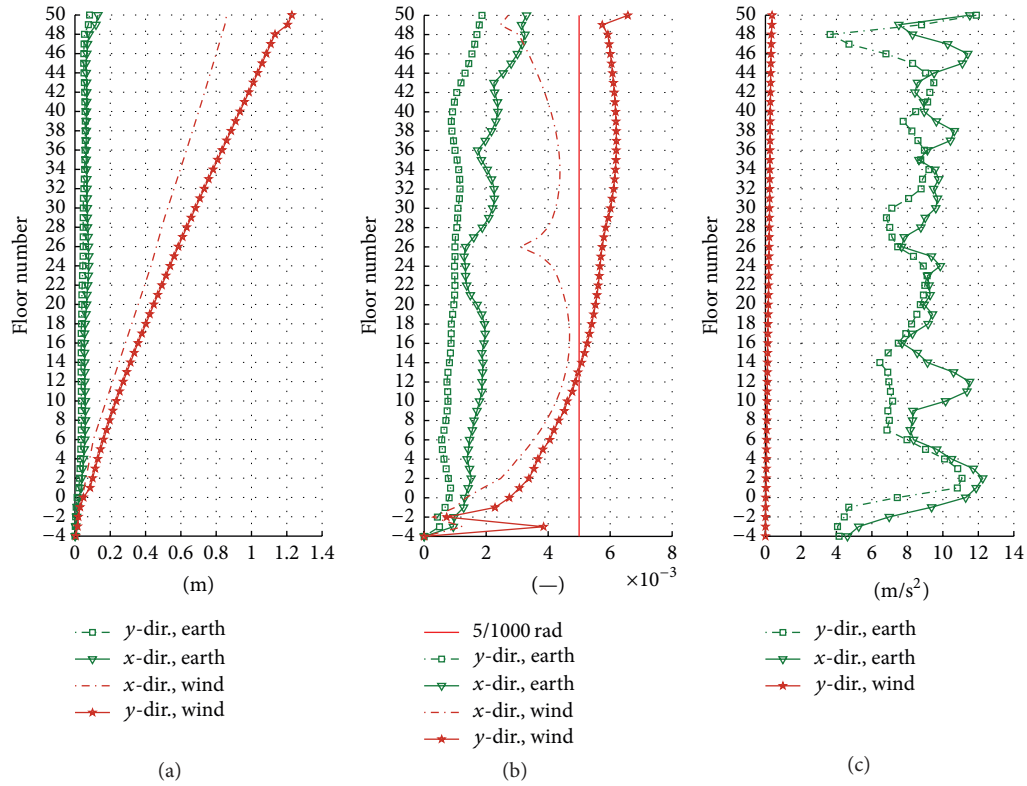

Figure 17: Peak responses of the 54-story building under wind and earthquake loads (not simultaneously): (a) displacement, (b) drift, and (c) acceleration.

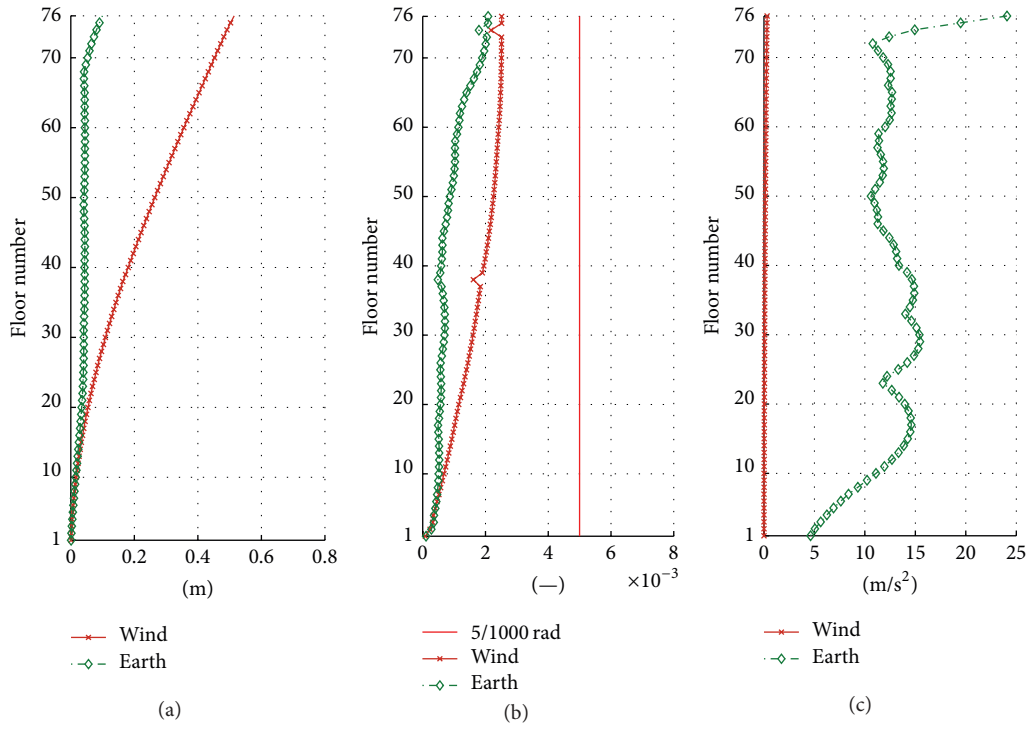

Figure 18: Peak responses of the 76-story building under wind and earthquake loads (not simultaneously): (a) displacement, (b) drift, and (c) acceleration. Note that the peak acceleration response at floor 75 (under wind loads) is 30 milli-g (this raises comfort and serviceability issues).

building needs control for both wind and earthquake impact reduction.

5. Mitigation Techniques

5.1. The Role of Damping. It was shown that the wind-induced responses of the tower are out of the comfort and security limits. This means that it is important to produce damping in the building in order to reduce its response. Damping is the dissipation of energy from an oscillating system, primarily through friction. The kinetic energy is transformed into heat.

Although finite element software packages can help to provide mode shapes, modal masses, and modal frequencies of the desired modes, they do not provide information about damping in buildings. This is because, unlike mass and rigidities that are distributed in a well-known matter along the elements, damping however is related to friction between joints and some hysteresis in the material which is difficult to be modeled. However, there is no convenient mean to refine the predictive capabilities regarding inherent structural damping, owing to its association with a number of complex mechanisms and even nonstructural elements.

Unlike the uncertainty in the stiffness, uncertainty in structural damping is comparatively high. However, while the main objective of adding damping via specially engineered components is to reduce building motion and in some cases design loads, a good effect is that the uncertainty in damping level can also be reduced.

The main current of structural technology is about to change from conventional earthquake-resistant structures which are designed "not to collapse even under the strongest earthquake" to controlled structures which are intended "to suppress the vibration itself." The concept of employing structural control to minimize structural vibration was proposed in the 1970s [53]. Structural control is a diverse field of study. Structural control is one area of current research that looks promising in attaining reduced structural vibrations during loadings such as earthquakes and strong winds. Structural control based on various passive, active, hybrid, and semiactive control schemes offers attractive opportunities to mitigate damage and loss of serviceability caused by natural hazards. The reducing of structural vibrations occurs by adding a mechanical system that is installed in a structure. The control of structural vibrations can also be done by various means such as modifying rigidities, masses, damping, or shape and by providing passive or active counter forces [54]. McNamara [55] studied the tuned mass damper (TMD) as an energy-absorbing system to reduce wind-induced structural response of buildings in the elastic range of behavior. Active control techniques are studied intensively for the control of the response of tall buildings under wind loads [56–62]. The most commonly used active control device for civil engineering structures is the active tuned mass damper (ATMD).

5.2. Robust Tuned Mass Dampers. Tuned mass dampers (TMDs) are used in both x- and y-directions. Although the mass of the TMD in the y-direction is taken as 3% of the first modal mass, it is still unable to satisfy the comfort criteria required. To overcome this problem, an actuator is added to the TMD to form an active tuned mass damper (ATMD). ATMD is used in the y-direction in order to improve the performance and the robustness of the TMD. Both LQG and fuzzy logic controllers are used to provide the optimal control force for the ATMD. Robustness and effectiveness of the fuzzy Logic controller over the LQG controller will be addressed.

The aim of the study presented in Aly [63] and Aly et al. [64] was to control the responses of the high-rise building under the wind loads measured in the wind tunnel using both TMDs and ATMDs. Active control of the structure using LQG and fuzzy logic controllers under wind that is attacking from different directions is studied. Lateral responses of the building in the two directions are controlled simultaneously while the effect of the uncontrolled torsional responses of the structure is considered instantaneously. A good reduction in the response of the building is obtained with both TMDs and ATMDs. Fuzzy logic controller has proved its robustness and the requirement of lower control forces over the LQG controller.

5.3. Magnetorheological Fluid Dampers. In recent years magnetorheological (MR) dampers have been verified with the unique ability to create the resisting force following the change of various characteristics. In Aly et al. [65, 66], MR dampers are placed in the tower as an alternative to TMDs and ATMD to reduce the wind-induced responses. The challenge in using such devices in tall buildings is related to where to put the device in the building. Unlike short and shear buildings, in which floor rotational angles are relatively small and there is a significant interstory drift under dynamic loads, slender tall buildings, however, may behave like a cantilever. Cantilever-like behaviour of buildings hinders the design of an effective internal bracing system. As shown in Figure 20, the building under consideration is shown to behave in one lateral direction like shear buildings (x-direction) and in the other direction as cantilever structures (y-direction). For the x-direction, internal bracings with MR dampers are used while for the y-direction outer bracings with MR dampers are proposed. Since the displacement across the damper is shown to be small, a lever mechanism is proposed for motions magnification. Both passive-on and decentralized bang-bang controllers showed that MR dampers with the proposed lever mechanism are effective in reducing the responses of the tower under wind loads in the two lateral directions.

Although TMDs and ATMD are shown to be effective in the response reduction of tall buildings under wind loads, they are large and heavy and take up valuable space at the top of the building. Moreover, they are an additional cost to the project (see Figure 19).

Viscous dampers and semiactive dampers can be used as alternatives to overcome these problems. These devices do not require frequency tuning, and while there is an optimum resistance characteristic for each application, the overall damping achieved is usually insensitive to the exact resistance characteristic of the device [37]. It is therefore sometimes possible to damp several modes with one device. The benefits of using dampers in tall buildings under wind loads are discussed in Hart and Jain [67]. Magnetorheological

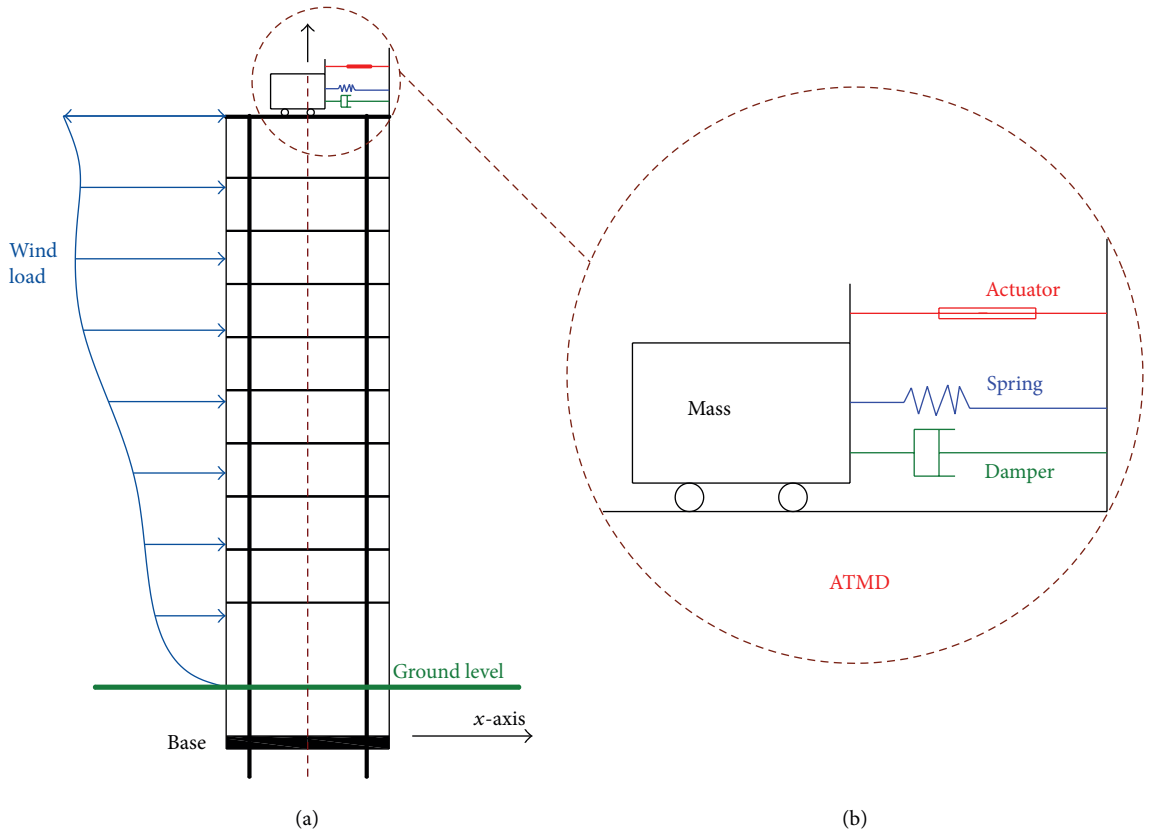

Figure 19: Active tuned mass damper (ATMD) installed on a tall building subjected to wind load: (a) location at the top of the building; (b) components of the ATMD.

dampers were used to reduce the acceleration and the design loads of the tower in the two lateral directions ([65, 66], see Figure 20). The authors are currently investigating proper techniques that can be used for mitigation under multihazard loading brought by both wind and earthquakes.

6. Discussion

It is important to mention that, even if the interstory drift ratios in tall buildings may be relatively small with no significant risk issues for the main force resisting system of the structure, nonstructural systems represent a high percentage of loss exposure of buildings to earthquakes. For instance, the *ceiling-piping-partition* system may be exposed to significant damage under earthquakes. Past earthquakes and numerical modeling considering potential earthquake scenarios show that the damage to this system causes the preponderance of US earthquake related losses [68, 69].

In the last two centuries, some major structural failures due to winds have occurred. Large structures have experienced failures as well, for example, the collapse of the Ferry bridge cooling towers in the UK in 1965 and the permanent deformation of the columns of the Great Plains Life Building in Lubbock, Texas, during a tornado (1970). Moreover, many super tall buildings have been seen to suffer from wind loads leading to structural annoying vibrations that cause, sometimes, horrible effects on the occupants. Such phenomenon needs a deep understanding in order to allow for providing adequate solutions.

Structural response prediction and reduction form an integral part of the building design process, providing architects and design engineers with a comprehensive understanding of the interaction between environmental factors and building design. A proper connotation of this interaction can provide significant cost savings to building owners in terms of developmental, material, and operational costs. This will expose them to the methods and procedures for the efficient application of wind studies in designing a building more economically than a similar building designed with more conservative building code provisions.

By doing so, the dynamic response of the building to wind effects (buffeting and vortex shedding) is virtually eliminated, leading to substantially reduced lateral design forces and ensuring occupant comfort. Substantial reductions in structural member size and construction cost savings can be realized in many cases. This may significantly improve the economic viability and sustainability of a development.

The safety and sustainability of buildings under wind and seismic hazards are a major concern, and it is a challenge for both the government and building owners. There is an argument to develop a decision support tool to assist decision-makers in the mitigation and retrofitting of buildings for multihazard environments, to improve the safety and sustainability of buildings. Potential damping

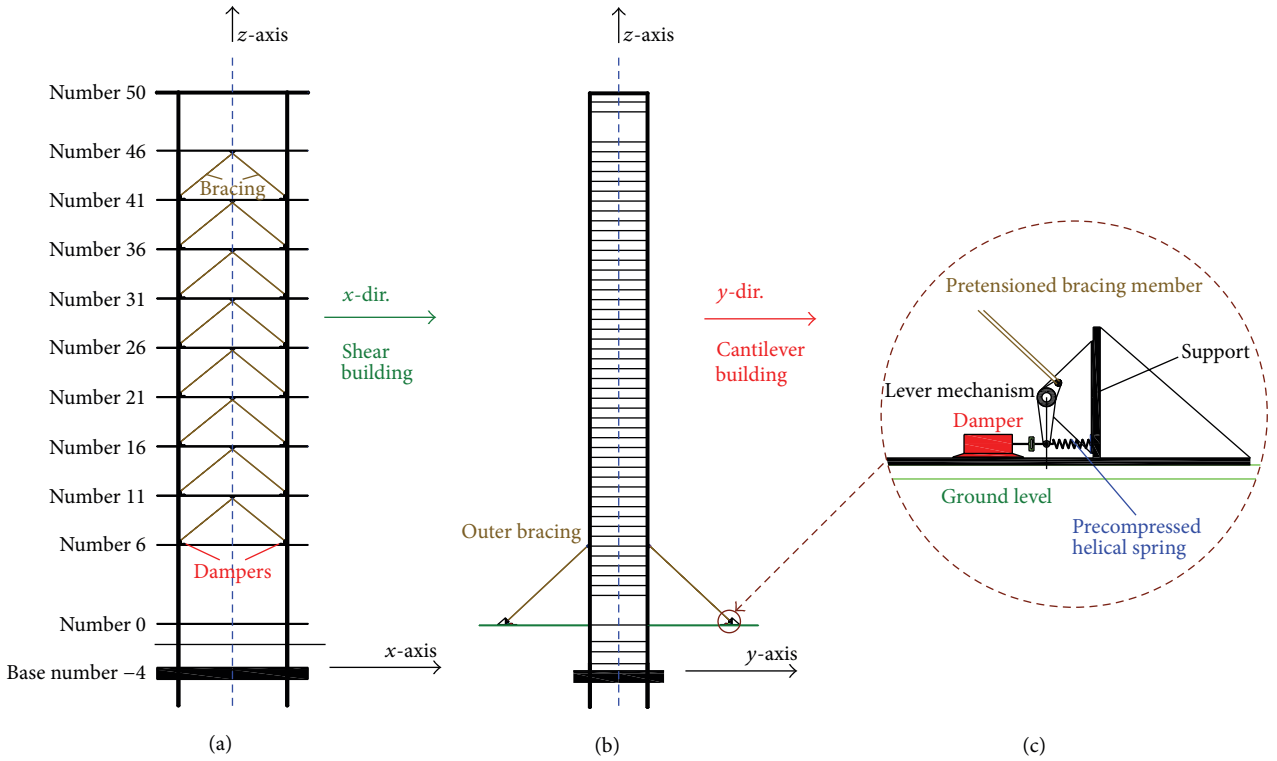

FIGURE 20: Proposed configuration of the MR dampers with bracing system: (a) bracings with dampers between adjacent floors for shear buildings; (b) outer bracings with dampers for cantilever and slender buildings; (c) damping unit consisting of a viscous damper, helical spring, and a lever mechanism for drift amplification across the damper.

solutions, in terms of selecting and implementing strategies to mitigate damages and minimize the consequences of failure, are therefore needed. It is envisaged that using a proper mitigation framework, and incorporating real-time data, a decision making tool for resilient and sustainable buildings can be developed. This will lead to sustainable solutions that can improve the performance of buildings under wind/earthquakes, reduce building life cycle costs, and increase efficiency in design.

7. Conclusions

The main objective of the current study was to further the understanding of the impact of multihazard loading, brought by wind and earthquakes, on the behavior of high-rise buildings, in order to apply such knowledge to design. The main contributions of the current study are summarized as follows:

(i) For dynamics and response under wind loads, general agreements between the results of the pressure integration technique and the aeroelastic experiment exist. However, the effect of the aerodynamic damping on the worst responses of a 54-story building in the two lateral directions is shown to be positive, which resulted in partial response reduction. Keeping in mind the complexity and the time required to prepare the aeroelastic model and to run the experiment, the pressure integration technique with FEM is recommended for such type of structures. Another advantage of the pressure integration technique is that a single model used in a single testing session can produce both overall structural loads and cladding loads.

(ii) The study shows that it is advantageous to predict the responses of tall buildings in their preliminary design stages as this can provide an opportunity to rotate the building to an optimal orientation that can lead to significant reduction in the responses. The results show that the worst peak acceleration is reduced by 38.5%, by rotating the building (54-story building) to a suggested orientation. This reduction is achieved without adding any structural elements/components to the primary building (no additional cost).

(iii) The results show that wind and earthquake loads are different from each other and are also different from static loads. This comes from the spectral comparison of the response of a high-rise building under the two types of excitation. The results indicate that earthquake loads excite higher modes that produce less interstory drift but higher acceleration which occurs for a relatively short time (compared to wind loads). Similar conclusions are obtained with both the 54-story and the 76-story buildings.

(iv) Although the acceleration under wind loads is lower than that under earthquake loads, it occurs for longer

periods that become a comfort issue. However, the drift under wind is larger which raises security issues. Similar conclusions are obtained with both the 54-story and the 76-story buildings.

(v) It seems that tall buildings designed for wind are safe under moderate earthquake loads. Nevertheless, it is important to mention that, even if the interstory drift ratios in tall buildings may be relatively small with no significant apparent issues for the main force resisting system of the structure, nonstructural systems may represent a high percentage of loss exposure of buildings to earthquakes due to high floor acceleration. Accordingly, appropriate damping techniques are recommended for response reduction under wind and earthquake loads.

The authors are currently investigating proper control techniques that can be used for response mitigation in tall buildings under multihazard loading.

Conflict of Interests

The authors declare that there is no conflict of interests regarding the publication of this paper.

Acknowledgments

The first author would like to acknowledge the support he received from PoliMI. Many thanks are due to the wind tunnel's research team for the help received, while participating in the experimental testing.

References

[1] Y. Li, A. Ahuja, and J. E. Padgett, "Review of methods to assess, design for, and mitigate multiple hazards," *Journal of Performance of Constructed Facilities*, vol. 26, no. 1, pp. 104–117, 2012.

[2] E. Y. Chen, *Multi-hazard design of mid-to high-rise structures [M.S. thesis]*, University of Illinois, 2012.

[3] L. Bullard, *The Empire State Building*, Lerner Publications, 2011.

[4] A. Frej and W. D. Browning, *Green Office Buildings: A Practical Guide to Development*, Urban Land Institute, Washington, DC, USA, 2005.

[5] A. M. Aly, "Design of buildings for wind and earthquake," in *Proceedings of the World Congress on Advances in Civil, Environmental, and Materials Research (ACEM '14)*, Busan, Republic of Korea, August 2014.

[6] M. Gu, H. L. Cao, and Y. Quan, "Experimental study of across-wind aerodynamic damping of super high-rise buildings with aerodynamically modified square cross-sections," *The Structural Design of Tall and Special Buildings*, vol. 23, no. 16, pp. 1225–1245, 2014.

[7] E. Dragomirescu and Y. Tun, "Modular repetitive structures as countermeasure to galloping," in *Proceedings of the International Conference on Advances in Wind and Structures (AWAS '14)*, Seoul, Republic of Korea, August 2014.

[8] K. Y. Billah, "Resonance, Tacoma Narrows bridge failure, and undergraduate physics textbooks," *The American Journal of Physics*, vol. 59, no. 2, pp. 118–124, 1991.

[9] J. A. Amin and A. K. Ahuja, "Mean interference effects between two buildings: Effects of close proximity," *The Structural Design of Tall and Special Buildings*, vol. 20, no. 7, pp. 832–852, 2011.

[10] P. Mendis, T. Ngo, N. Haritos, A. Hira, B. Samali, and J. Cheung, "Wind loading on tall buildings," *EJSE Special Issue: Loading on Structures*, vol. 3, pp. 41–54, 2007.

[11] A. G. Davenport, "The dependence of wind loads on meteorological parameters," in *Proceedings of the International Research Seminar on Wind Effects on Buildings and Structures*, pp. 19–82, University of Toronto Press, Ottawa, Canada, September 1967.

[12] D. J. Johns, "Wind excited behavior of structures," *The Shock and Vibration Digest*, vol. 8, no. 4, pp. 67–75, 1976.

[13] D. J. Johns, "Wind excited behavior of structures II," *The Shock and Vibration Digest*, vol. 11, no. 4, pp. 17–29, 1979.

[14] A. M. Aly, *On the dynamics of buildings under winds and earthquakes: response prediction and reduction [Ph.D. thesis]*, Department of Mechanical Engineering, Politecnico di Milano, Milano, Italy, 2009.

[15] ASCE 7-2010, "Minimum design loads for buildings and other structures," ASCE Standard ASCE/SEI 7-10, American Society of Civil Engineers, Reston, Va, USA, 2010.

[16] European Standard, "Eurocode 1. Actions on structures—Part 1–4: general actions—wind actions," prEN 1991-1-4, European Standard, 2004.

[17] A. Kareem, "Dynamic response of high-rise buildings to stochastic wind loads," *Journal of Wind Engineering and Industrial Aerodynamics*, vol. 42, no. 1–3, pp. 1101–1112, 1992.

[18] A. Kareem, "Aerodynamic response of structures with parametric uncertainties," *Structural Safety*, vol. 5, no. 3, pp. 205–225, 1988.

[19] Y. Zhou, T. Kijewski, and A. Kareem, "Aerodynamic loads on tall buildings: interactive database," *Journal of Structural Engineering*, vol. 129, no. 3, pp. 394–404, 2003.

[20] NatHaz, Aerodynamic Loads Database, 2008, http://aerodata.ce.nd.edu/.

[21] A. Kareem and J. E. Cermak, "Wind tunnel simulation of wind structure interactions," *ISA Transactions*, vol. 18, no. 4, pp. 23–41, 1979.

[22] D. W. Boggs and J. A. Peterka, "Aerodynamic model tests of tall buildings," *Journal of Engineering Mechanics*, vol. 115, no. 3, pp. 618–635, 1989.

[23] A. M. Aly, "Pressure integration technique for predicting wind-induced response in high-rise buildings," *Alexandria Engineering Journal*, vol. 52, no. 4, pp. 717–731, 2013.

[24] A. Zasso, A. M. Aly, L. Rosa, and G. Tomasini, "Wind induced dynamics of a prismatic slender building with 1:3 rectangular section," in *Proceedings of the BBAA VI International Colloquium on Bluff Bodies Aerodynamics & Applications*, Milano, Italy, July 2008.

[25] C. J. Ammon, *EAS-A193 Class Notes*, 2015, http://eqseis.geosc.psu.edu/~cammon/HTML/Classes/IntroQuakes/Notes/earthquake_effects.html.

[26] R. J. Geller, D. D. Jackson, Y. Y. Kagan, and F. Mulargia, "Enhanced: earthquakes cannot be predicted," *Science*, vol. 275, no. 5306, pp. 1616–1620, 1997.

[27] H. Kanamori, E. Hauksson, and T. Heaton, "Real-time seismology and earthquake hazard mitigation," *Nature*, vol. 390, no. 6659, pp. 461–464, 1997.

[28] K. Vranes and R. Pielke Jr., "Normalized earthquake damage and fatalities in the united states: 1900–2005," *Natural Hazards Review*, vol. 10, no. 3, pp. 84–101, 2009.

[29] Eurocode 8, "Design of structures for earthquake resistanc—part 1: general rules, seismic actions and rules for buildings," European Standard prEN 1998-1, 2003.

[30] G. Koulouras, G. Balasis, I. Kiourktsidis et al., "Discrimination between pre-seismic electromagnetic anomalies and solar activity effects," *Physica Scripta*, vol. 79, no. 4, Article ID 045901, 2009.

[31] F. A. Potra and E. Simiu, "Multihazard design: structural optimization approach," *Journal of Optimization Theory and Applications*, vol. 144, no. 1, pp. 120–136, 2010.

[32] D. Duthinh and E. Simiu, "Safety of structures in strong winds and earthquakes: multihazard considerations," *Journal of Structural Engineering*, vol. 136, no. 3, pp. 330–333, 2010.

[33] C. Crosti, D. Duthinh, and E. Simiu, "Risk consistency and synergy in multihazard design," *Journal of Structural Engineering*, vol. 137, no. 8, pp. 844–849, 2011.

[34] Y. Li and B. R. Ellingwood, "Framework for multihazard risk assessment and mitigation for wood-frame residential construction," *Journal of Structural Engineering*, vol. 135, no. 2, pp. 159–168, 2009.

[35] B. C. Huang, K. M. Lam, A. Y. T. Leung, and Y. K. Cheung, "Equivalent modal damping ratios of a composite tube-type tail building to dynamic wind loading," *Shock and Vibration*, vol. 3, no. 2, pp. 99–105, 1996.

[36] N. Satake, K.-I. Suda, T. Arakawa, A. Sasaki, and Y. Tamura, "Damping evaluation using full-scale data of buildings in Japan," *Journal of Structural Engineering*, vol. 129, no. 4, pp. 470–477, 2003.

[37] R. J. Smith and M. R. Willford, "The damped outrigger concept for tall buildings," *Structural Design of Tall and Special Buildings*, vol. 16, no. 4, pp. 501–517, 2007.

[38] Y. Tamura and A. Yoshida, "Amplitude dependency of damping in buildings," in *Proceedings of the 18th Analysis and Computation Specialty Conference*, Vancouver, Canada, April 2008.

[39] S. Attaway, *Matlab: A Practical Introduction to Programming and Problem Solving*, Butterworth-Heinemann, Amsterdam, The Netherlands, 2009.

[40] A. M. Aly, "Proposed approach for determination of tributary areas for scattered pressure taps," *Wind and Structures*, vol. 16, no. 6, pp. 617–627, 2013.

[41] E. Simiu and R. H. Scanlan, *Wind Effects on Structures: Fundamentals and Applications to Design*, John Wiley & Sons, New York, NY, USA, 1996.

[42] G. Diana, S. Giappino, F. Resta, G. Tomasini, and A. Zasso, "Motion effects on the aerodynamic forces for an oscillating tower through wind tunnel tests," in *Proceedings of the 5th European and African Conference on Wind Engineering*, pp. 53–56, Florence, Italy, 2009.

[43] ASCE, *Wind Tunnel Studies of Buildings and Structures*, ASCE Manuals and Reports of Engineering Practice no. 67, American Society of Civil Engineers, Reston, Va, USA, 1999.

[44] A. M. Aly, *Vibration control in structures due to earthquake effects using MR damper [M.S. thesis]*, Department of Mechanical Engineering, Alexandria University, Alexandria, Egypt, 2005.

[45] H. M. Metwally, B. M. El-Souhily, and A. Aly, "Reducing vibration effects on buildings due to earthquake using magneto-rheological dampers," *Alexandria Engineering Journal*, vol. 45, no. 2, pp. 131–140, 2006.

[46] A. M. Aly and R. E. Christenson, "On the evaluation of the efficacy of a smart damper: a new equivalent energy-based probabilistic approach," *Smart Materials and Structures*, vol. 17, no. 4, Article ID 045008, 11 pages, 2008.

[47] Gazzetta Ufficiale, "Supplemento n. 72 della Gazzetta Ufficiale n. 105 del 08.05.2003," 2003, (Italian).

[48] I. Chowdhury and S. Dasgupta, "Computation of Rayleigh damping coefficients for large systems," *The Electronic Journal of Geotechnical Engineering*, vol. 8, Bundle 8C, 2003.

[49] L. Meirovitch, *Analytical Methods in Vibrations*, The MacMillan, New York, NY, USA, 1967.

[50] J. N. Yang, J. C. Wu, B. Samali, and A. K. Agrawal, "A benchmark problem for response control of wind-excited tall buildings," in *Proceedings of the 2nd World Conference on Structural Control*, vol. 2, pp. 1407–1416, Wiley, New York, NY, USA, 1998.

[51] J. N. Yang, A. K. Agrawal, B. Samali, and J.-C. Wu, "Benchmark problem for response control of wind-excited tall buildings," *Journal of Engineering Mechanics*, vol. 130, no. 4, pp. 437–446, 2004.

[52] H. Kim and H. Adeli, "Wind-induced motion control of 76-story benchmark building using the hybrid damper-TLCD system," *Journal of Structural Engineering*, vol. 131, no. 12, pp. 1794–1802, 2005.

[53] J. T. P. Yao, "Concept of structural control," *ASCE Journal of Structural Engineering*, vol. 98, no. 7, pp. 1567–1574, 1972.

[54] G. W. Housner, L. A. Bergman, T. K. Caughey et al., "Structural control: past, present, and future," *Journal of Engineering Mechanics*, vol. 123, no. 9, pp. 897–971, 1997.

[55] R. J. McNamara, "Tuned mass dampers for buildings," *ASCE Journal of the Structural Division*, vol. 103, no. 9, pp. 1785–1798, 1977.

[56] T. T. Soong, *Active Structural Control: Theory and Practice*, Longman, 1990.

[57] R. J. Facioni, K. C. S. Kwok, and B. Samali, "Wind tunnel investigation of active vibration control of tall buildings," *Journal of Wind Engineering and Industrial Aerodynamics*, vol. 54-55, pp. 397–412, 1995.

[58] M. Gu and F. Peng, "An experimental study of active control of wind-induced vibration of super-tall buildings," *Journal of Wind Engineering and Industrial Aerodynamics*, vol. 90, no. 12–15, pp. 1919–1931, 2002.

[59] J.-C. Wu and B.-C. Pan, "Wind tunnel verification of actively controlled high-rise building in along-wind motion," *Journal of Wind Engineering & Industrial Aerodynamics*, vol. 90, no. 12–15, pp. 1933–1950, 2002.

[60] L.-T. Lu, W.-L. Chiang, J.-P. Tang, M.-Y. Liu, and C.-W. Chen, "Active control for a benchmark building under wind excitations," *Journal of Wind Engineering and Industrial Aerodynamics*, vol. 91, no. 4, pp. 469–493, 2003.

[61] X. Lu, P. Li, X. Guo, W. Shi, and J. Liu, "Vibration control using ATMD and site measurements on the Shanghai World Financial Center Tower," *The Structural Design of Tall and Special Buildings*, vol. 23, no. 2, pp. 105–123, 2014.

[62] Ş. S. Özsariyildiz and A. Bozer, "Finding optimal parameters of tuned mass dampers," *The Structural Design of Tall and Special Buildings*, vol. 24, no. 6, pp. 461–475, 2015.

[63] A. M. Aly, "Proposed robust tuned mass damper for response mitigation in buildings exposed to multidirectional wind," *Structural Design of Tall and Special Buildings*, vol. 23, no. 9, pp. 664–691, 2014.

[64] A. M. Aly, F. Resta, and A. Zasso, "Active control in a high-rise building under multidirectional wind loads," *Smart Materials Research*, vol. 2011, Article ID 549621, 15 pages, 2011.

[65] A. M. Aly, A. Zasso, and F. Resta, "On the dynamics of a very slender building under winds: response reduction using MR dampers with lever mechanism," *Structural Design of Tall and Special Buildings*, vol. 20, no. 5, pp. 539–551, 2011.

[66] A. M. Aly Sayed Ahmed, A. Zasso, and F. Resta, "Proposed configurations for the use of smart dampers with bracings in tall buildings," *Smart Materials Research*, vol. 2012, Article ID 251543, 16 pages, 2012.

[67] G. C. Hart and A. Jain, "Performance-based wind evaluation and strengthening of existing tall concrete buildings in the los angeles region: dampers, nonlinear time history analysis and structural reliability," *The Structural Design of Tall and Special Buildings*, vol. 23, no. 16, pp. 1256–1274, 2014.

[68] J. Weiser, G. Pekcan, E. Zaghi, A. Itani, and M. Maragakis, "Floor acceleration in yielding SMRF structures," *Earthquake Spectra*, vol. 29, no. 3, pp. 987–1002, 2013.

[69] A. E. Zaghi, E. M. Maragakis, A. Itani, and E. Goodwin, "Experimental and analytical studies of hospital piping assemblies subjected to seismic loading," *Earthquake Spectra*, vol. 28, no. 1, pp. 367–384, 2012.